All in One and One for All: A Simple yet Effective Method towards Cross-domain Graph Pretraining

Haihong Zhao*
Data Science and Analytics Thrust,
The Hong Kong University of Science
and Technology (Guangzhou)
Guangzhou, China
hzhaobf@connect.ust.hk

Aochuan Chen*
Data Science and Analytics Thrust,
The Hong Kong University of Science
and Technology (Guangzhou)
Guangzhou, China
achen149@connect.hkust-gz.edu.cn

Xiangguo Sun*†
Department of Systems Engineering
and Engineering Management, and
Shun Hing Institute of Advanced
Engineering, The Chinese University
of Hong Kong
Hong Kong SAR, China
xgsun@se.cuhk.edu.hk

Hong Cheng

Department of Systems Engineering and Engineering Management, and Shun Hing Institute of Advanced Engineering, The Chinese University of Hong Kong Hong Kong SAR, China hcheng@se.cuhk.edu.hk

Iia Li[†]

Data Science and Analytics Thrust, The Hong Kong University of Science and Technology (Guangzhou) Guangzhou, China jialee@ust.hk

ABSTRACT

Large Language Models (LLMs) have revolutionized the fields of computer vision (CV) and natural language processing (NLP). One of the most notable advancements of LLMs is that a single model is trained on vast and diverse datasets spanning multiple domains - a paradigm we term 'All in One'. This methodology empowers LLMs with super generalization capabilities, facilitating an encompassing comprehension of varied data distributions. Leveraging these capabilities, a single LLM demonstrates remarkable versatility across a variety of domains - a paradigm we term 'One for All'. However, applying this idea to the graph field remains a formidable challenge, with cross-domain pretraining often resulting in negative transfer. This issue is particularly important in few-shot learning scenarios, where the paucity of training data necessitates the incorporation of external knowledge sources. In response to this challenge, we propose a novel approach called Graph COordinators for PrEtraining (GCOPE), that harnesses the underlying commonalities across diverse graph datasets to enhance few-shot learning. Our novel methodology involves a unification framework that amalgamates disparate graph datasets during the pretraining phase to distill and transfer meaningful knowledge to target tasks. Extensive experiments across multiple graph datasets demonstrate the superior

Permission to make digital or hard copies of all or part of this work for personal or classroom use is granted without fee provided that copies are not made or distributed for profit or commercial advantage and that copies bear this notice and the full citation on the first page. Copyrights for components of this work owned by others than the author(s) must be honored. Abstracting with credit is permitted. To copy otherwise, or republish, to post on servers or to redistribute to lists, requires prior specific permission and/or a fee. Request permissions from permissions@acm.org.

KDD '24, August 25–29, 2024, Barcelona, Spain

© 2024 Copyright held by the owner/author(s). Publication rights licensed to ACM. ACM ISBN 979-8-4007-0490-1/24/08

https://doi.org/10.1145/3637528.3671913

efficacy of our approach. By successfully leveraging the synergistic potential of multiple graph datasets for pretraining, our work stands as a pioneering contribution to the realm of graph foundational model. Code available at https://github.com/cshhzhao/GCOPE.

CCS CONCEPTS

Computing methodologies → Transfer learning.

KEYWORDS

pretraining; prompt tuning; graph neural networks

ACM Reference Format:

Haihong Zhao, Aochuan Chen, Xiangguo Sun, Hong Cheng, and Jia Li. 2024. All in One and One for All: A Simple yet Effective Method towards Cross-domain Graph Pretraining. In *Proceedings of the 30th ACM SIGKDD Conference on Knowledge Discovery and Data Mining (KDD '24), August 25–29, 2024, Barcelona, Spain.* ACM, New York, NY, USA, 12 pages. https://doi.org/10.1145/3637528.3671913

1 INTRODUCTION

Recently, artificial general intelligence (AGI) has achieved remarkable advancement in the realms of computer vision (CV) [2, 4, 31, 48] and natural language processing (NLP) [6, 39]. One of the key innovations for these models is that they pre-train one foundation model through various contexts, making the model absorb and synthesize knowledge across diverse domains (a.k.a "all in one") to deliver robust, context-aware responses. Their ability to generalize and apply learned knowledge to a wide spectrum of downstream domains (a.k.a "one for all") is a testament to the success of their pre-training strategies, which effectively capture and utilize the nuances across different domains.

Compared with NLP and CV areas, graph data is non-linear and more general. For example, a sentence can be seen as a graph path

^{*}Equal Contribution.

[†]Corresponding author.

and an image can be seen as a grid graph. These observations indicate a broader and more ambitious goal of a more generalized and versatile artificial intelligence by graphs. However, pre-training on graphs is still grappling with the integration of multi-domain knowledge and cross-domain generalization. Although existing graph transfer learning methods [18, 26, 36, 37, 49, 52] demonstrate proficiency within the same domain, their successes, often confined to transferring tasks within a similar graph dataset, exhibit inherent limitations when attempting to transcend the graph domain boundary. These disparities make it difficult for graph models to replicate the success of their NLP and CV counterparts, yet the pursuit of moving beyond existing domain-specific task transferring and towards a more versatile approach is not just an extension of existing methodologies but a stride towards bridging the gap between domain-specific proficiency and the broader vision of general artificial intelligence.

However, achieving this vision is very intractable. The first challenge lies in the diversity of structural patterns, which is particularly observed between homophilic graphs (a pair of nodes are intended to be similar if they are connected) and heterophilic graphs (connected nodes depart from each other). Graphs inherently exhibit diverse topologies and features, making it challenging to identify and leverage common patterns across different domains. The good thing is that this diversity enriches the external knowledge and contains huge potential for more general transferability to various downstream applications. However, it also complicates the task of identifying and leveraging commonalities across domains, as models must balance the fine line between capturing the essence of individual graphs and maintaining the generalization across different datasets.

The second challenge is the complexity inherent in aligning semantic spaces (features) across different graph datasets. Unlike domains with a structured, common framework (like images or texts), graph data is diverse and abstract. Features in one graph might have no direct counterpart in another, making it incredibly challenging to align these features in a meaningful way. This alignment is not just a matter of mapping features but of understanding and reconciling the underlying semantics and contexts they represent. The absence of a universal framework to guide this alignment makes it a daunting task, one that requires a sophisticated approach to bridge the gap between disparate graph datasets effectively. Some recent works [22] are trying to align different graph semantic spaces by generating a textual description of these graphs and then using LLMs to learn a unified representation, but they can only deal with text-attributed graphs or graphs with specific feature semantics. In a broader range, many graphs have only latent feature vectors and we actually do not know how exactly each dimension means, let alone generate a textual description.

Inspired by recent achievements of graph prompt [36], which has been carefully demonstrated as a powerful approach to manipulate various graph data, we hope to introduce the graph prompting technique to conduct more advanced operations on different graph datasets, to bridge the gap left by cross-domain graph pretraining and transferring. Specifically, we introduce the concept of "coordinators", which are some virtual nodes that function as dynamic bridges between disparate graph datasets. These coordinators share the same theory foundation of graph prompts that

have the powerful capability of data manipulation. The theory foundation ensures that these coordinators can learn an appropriate latent data manipulation strategy to harmonize different datasets, promote a unified representation, and adapt to the specificities of each graph, thus ensuring that the model doesn't just see a collection of isolated datasets but a harmonious, interconnected network. This innovation allows the model to navigate the diversity of graph structures adeptly, recognizing and leveraging underlying commonalities and differences in a balanced and informed manner. Beyond the coordinators, we also design a complete pretraining framework and provide two transferring components, which can ensure that the knowledge transferred is not just relevant but also contextually enriched, turning potential negative transfer into a positive, performance-enhancing phenomenon. In summary, the main contributions are as follows:

- We propose a very simple yet very effective framework, named "GCOPE", as a novel mechanism to unify diverse graph structures, enabling the seamless integration and a unified graph pre-training framework, making the pre-trained graph model able to preserve multi-domain knowledge across different graph datasets.
- Inspired by the powerful data manipulation capability of graph prompts in the downstream stage, we propose similar "coordinators" in the pre-training stage so that we can learn a latent data alignment strategy and ensure the relevance and efficacy of knowledge transfer, especially in few-shot learning scenarios.
- Our pre-training framework is compatible with various graph pre-training methods and the transferring stage can also leverage both fine-tuning and prompting techniques.
- We conduct comprehensive experimental evaluation, the results from which demonstrate the superior performance of our approach across multiple graph datasets.

2 MOTIVATION

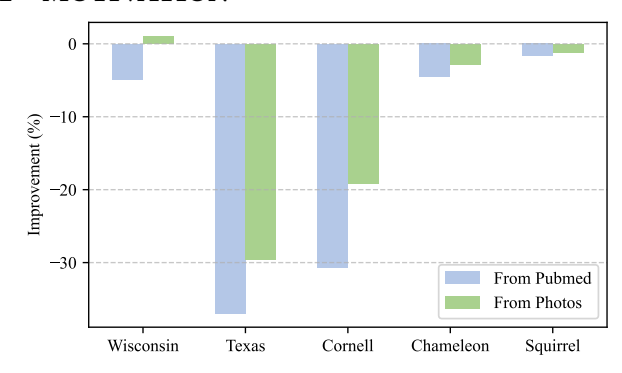


Figure 1: Negative transfer phenomenon in the single-source cross-domain transfer setting. Sources (Pubmed and Photos) are two homophilic datasets. Targets (Wisconsin, Texas, Cornell, Chameleon, and Squirrel) are five heterophilic graphs.

Unlike images, words, or sentences, which often share extensive underlying semantics across datasets, graph data are more abstract, making it more challenging to discern low-level common semantics. Therefore, the negative transfer phenomenon [20, 47] is commonly found in the field of graph learning. Here, we focus on the representative C-way-K-shot setting. We validate this phenomenon

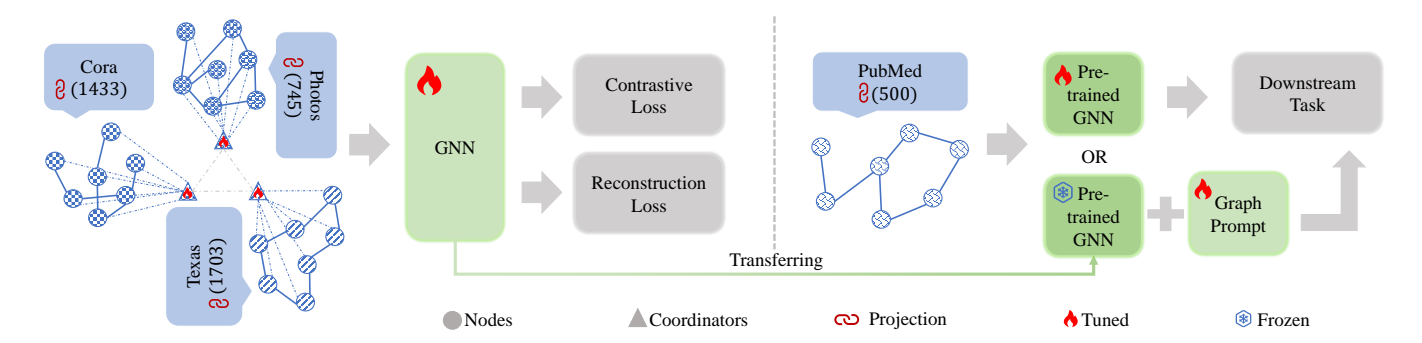


Figure 2: Overview of our proposed GCOPE method. The left part is our pretraining stage and the right part transferring stage.

through extensive experimentation, examining two main scenarios: the transfer of knowledge from a single source dataset, as well as from multiple source datasets.

Observations: As depicted in Figure 1, transferring from a single source dataset does indeed negatively affect the target task, confirming our analysis of the distinctiveness of two graph datasets. In order to overcome this obstacle, it is necessary to expand the scope of the source dataset so that it can offer valuable insights for the downstream task. However, a brutal combination of source datasets still failed to enhance the performance of the target task. We detail this in section 4.2.

Further Analysis: The first reason causing this negative transfer across domains is that the structural patterns are different, especially reflected in homophilic and heterophilic datasets. Graph data is characterized by its complex network of connections, where nodes are not isolated but part of an interconnected structure. The relationships among nodes, represented by edges, facilitate the flow of influence and information, making each node both a product and a contributor to its environment. This interconnectivity is central to graph data, resulting in systems where the collective properties surpass those of individual components. Nonetheless, this characteristic presents challenges for machine learning models that attempt to learn from multiple graph datasets simultaneously. Each dataset is akin to its own distinct ecosystem, governed by its unique topology and rules. Within a given graph, nodes and edges are attuned to specific patterns and linkages that are relevant within that context. When merging different graphs for joint training, the inherent disparity of each graph's structure becomes a barrier, as the datasets naturally exist in isolation from one another and thus the information flow is blocked.

The second reason is the lack of feature alignment across these datasets. Graph attributes are heterogeneous and context-dependent, representing a wide range of abstract concepts and connections. Unlike textual or visual data, which have a common reference framework, graph attributes are highly varied and specific to their domain. Consequently, aligning features from different graphs is a daunting task, as there is no straightforward method to reconcile the disparate languages of each dataset into a unified representation for machine learning models to process.

Objectives: In this paper, we focus on the above two challenges, the disparity and isolation of graph datasets and the difficulty in aligning their diverse features. We denote our pretraining datasets

as comprising M graphs, represented as $\mathcal{G}^{(i)} = (\mathcal{V}^{(i)}, \mathcal{E}^{(i)}), i \in \{1, 2, \cdots, M\}$, where $\mathcal{V}^{(i)} = \{v_1^{(i)}, v_2^{(i)}, \cdots, v_{|\mathcal{V}_i|}^{(i)}\}$ and $\mathcal{E}^{(i)} = \mathcal{V}^{(i)} \times \mathcal{V}^{(i)}$ denote the sets of nodes and edges, respectively. Each $\mathcal{G}^{(i)}$ is associated with feature matrix $X^{(i)} \in \mathbb{R}^{|\mathcal{V}^{(i)}| \times d_i}$ and adjacency matrix $A^{(i)} \in \mathbb{R}^{|\mathcal{V}^{(i)}| \times |\mathcal{V}^{(i)}|}$. Our objective is to train a GNN $h(\cdot)$ parameterized by Θ , which is capable of encoding knowledge transferable to downstream tasks. The downstream dataset is represented as $\mathcal{G}^{(t)} = (\mathcal{V}^{(t)}, \mathcal{E}^{(t)})$ with the feature matrix $X^{(t)}$ and adajcency matrix $A^{(t)}$. To address this question, we carefully design a general pretraining scheme that is independent of datasets, network architectures and downstream tasks.

3 METHOD

3.1 Overview of Our Framework

In this section, we introduce a cohesive approach that enables the simultaneous pretraining of a graph model on multiple datasets. We utilize established pretraining objectives, namely GraphCL [46] and SimGRACE [43], to guide the learning process. Additionally, we implement novel techniques specifically designed to overcome the challenges highlighted in Section 2. A visual representation of our methodology is provided in Figure 2.

3.2 Aligning Graphs by Coordinators

Different graphs usually have different features and structural patterns. Here we propose a two-phase graph alignment approach. The first step is to make the feature dimensions all the same in format. Then we seek to further learn a latent data alignment strategy by coordinators, which can reformulate graphs w.r.t their structural patterns and semantic patterns.

3.2.1 Feature Projection. During the pretraining phase of our GNN model, we first present a projecting module to align feature dimension, which is described by:

$$\tilde{X}^{(i)} = \operatorname{Proj}(X^{(i)}) \in \mathbb{R}^{|\mathcal{V}^{(i)}| \times d_{\mathcal{P}}}, \tag{1}$$

where $\operatorname{Proj}(\cdot)$ denotes a certain projection operation and d_{P} denotes the predefined projected dimension. Without loss of generality, we provide two widely used methods, singular value decomposition (SVD) and attention mechanism, as two representative projection operations in this paper. However, it is worth mentioning that the mere projection of features onto a common plane does not suffice to address the alignment challenge; additional alignment endeavors are indispensable.

3.2.2 Graph Coordinators. Based on the above step, we present a novel concept: virtual nodes, referred to herein as "coordinators". These coordinators are strategically crafted to enhance interconnectivity among disparate graphs, facilitating the alignment of their features and structural conflicts.

(i). Cross Connection between Coordinators and Datasets: To ensure that each graph retains its unique structural properties while still participating in a larger, interconnected system, we assign a dedicated coordinator to each graph dataset. This coordinator is not just a peripheral addition; it becomes an integral component of the graph by forming a fully connected subnetwork with every node within the graph to which it is assigned. This design choice ensures that the coordinator has an immediate, direct line of communication with each node, allowing it to efficiently relay information and coordinate interactions within its respective graph.

(ii). Inner Connection within Coordinators: However, our ambition extends beyond enhancing individual graph structures; we aim to facilitate a rich tapestry of connections spanning all graphs within our dataset collection. To achieve this, we strategically connect coordinators from different graphs. These inter-coordinator edges act as bridges, enabling the flow of information between disparate graphs that would otherwise remain siloed. As a result, we construct a comprehensive communication infrastructure that seamlessly integrates the entirety of the graph collection, fostering a new level of collaboration and knowledge sharing among them. With the above modification, we can get a joint adjacency matrix \tilde{A} , which consists of adjacency matrices of original graphs and new rows for coordinators. Mathematically, \tilde{A} can be defined as follows:

$$\tilde{A} = \begin{bmatrix} A_{\text{diag}} & R_A^T \\ R_A & R_R \end{bmatrix}, \tag{2}$$

where $A_{\mathrm{diag}} = \mathrm{Diag}(A^{(1)}, A^{(2)}, \cdots, A^{(M)}), \ R_R = \mathbf{1}^{M \times M}, \ R_A = \mathrm{Stack}(R_A^{(1)}, R_A^{(2)}, \cdots, R_A^{(M)}).$ Diag means concatenating matrices diagonally, and Stack means stacking row-vectors into a matrix. Specifically, $R_A^{(i)} \in \mathbb{R}^{\sum_k^M |\mathcal{V}^{(k)}|}$ and we have the jth value of $R_A^{(i)}$:

$$R_A^{(i)}(j) = \begin{cases} 1 & \sum_{1}^{i} |\mathcal{V}^{(k)}| \le j < \sum_{1}^{i+1} |\mathcal{V}^{(k)}| \\ 0 & \text{otherwise.} \end{cases}$$
 (3)

We treat the coordinator representation as learnable parameters. We opt for a flexible approach so that they can evolve organically alongside the GNN training, adapting dynamically to the data. This ensures they continually refine their attributes to effectively serve as conduits of evolving graph embeddings.

(iii). Generate Graph Batches for Efficient Training: Moreover, by harnessing the interconnectivity facilitated by coordinators, we unlock the potential for joint sampling of nodes originating from diverse data graphs. This innovative strategy empowers the training process through aggregated batches, thereby promoting the natural alignment of features across datasets. Exposing the model to a plethora of features within a single learning iteration prompts it to seek out unified representations, effectively synthesizing insights from disparate sources into cohesive and comprehensive representations. This unified approach not only enhances the model's ability to capture the underlying structure of the data but also fosters robust generalization across domains.

3.2.3 Why It Works? Kindly note that our proposed coordinators have the same theory support as graph prompts. The main difference is that general graph prompts are used for downstream tasks while we use coordinators during pretraining. Evidenced by [7, 36], prompts are demonstrated to be tantamount to graph transformations (e.g., node, edge, graph removing or adding, and some node feature operations). In parallel, our coordinators can be construed as a form of graph transformation. Given a GNN denoted as $g(\cdot)$ and a prompt p, it has been established that:

$$g(\tilde{X} + p, \tilde{A}) = g(t(\tilde{X}, \tilde{A})) + O_{ap}$$
(4)

where O_{gp} represents an error bound associated with the GNN $g(\cdot)$ and the prompt p. Here, $t(\cdot)$ signifies a graph transformation operation. Given that the learnable features embedded within our coordinators can be interpreted as the prompt p, they facilitate equivalent graph transformations for the originally isolated graphs. The learned equivalent transformation effectively harmonizes these graphs (e.g., homophilic and heterophilic graphs), enabling the discovery of inherent commonalities among them.

Additionally, we would like to facilitate a better understanding of our framework's design principles and the functions of its various components through 'Interdisciplinary Teaching', which is a cutting-edge approach in the field of education:

'Interdisciplinary Teaching' aims to enhance the comprehensiveness and depth of learning by integrating knowledge and methods from different subjects, similar to how GCOPE integrates diverse graph datasets. It addresses the complexity of real-world problems (like diverse and complex structures, attributes, and structure-attribute patterns), requiring a multidisciplinary perspective for solutions and encouraging students to apply cross-domain knowledge. This approach leads to a more thorough understanding and higher-level thinking skills, mostly like the transferrable pretrained graph representations. The integration strategy in education, which highlights core concepts and fosters interaction among disciplines, resembles the coordinators in GCOPE. This helps students see the bridges between subjects, nurturing flexible and innovative thinking, like transferring to new downstream datasets, especially the few-shot scenarios.

3.3 Pretraining on Multi-domain Graphs

Our approach is very flexible and compatible with many pretraining approaches. Here, we present a general pretraining framework that can extract high-quality embeddings at both the node and graph levels. Prior research has predominantly focused on pretraining within the same data domains as the downstream task [14]. Within this context, GraphCL [46] and SimGRACE [43] have been particularly noteworthy for their effectiveness in generating granular node embeddings as well as holistic graph embeddings. GraphCL employs graph data augmentation to generate positive pairs, whereas SimGRACE perturbs the GNN to achieve this objective. Given the strengths of these methods, we chose them as our basic pretraining strategy.

Next, we move on to the crucial task of preserving the integrity of information from each graph. To this end, we introduce an auxiliary feature reconstruction loss. This loss is quantified through the mean squared error (MSE) metric, which assesses the discrepancy between the original node feature vector (after projection)

 \hat{x}_i and the reconstructed feature vector \hat{x}_i . The latter is generated by applying a multilayer perceptron (MLP) to the embedded node representation h_i , thus enabling the evaluation of the fidelity with which the embedding process preserves the original node features. The purpose of this loss function is to ensure that, despite the projection of features, the salient and defining characteristics of each graph's information are retained and remain compatible. To be concrete, taking GraphCL as an example, our pretraining objective can be described as follows:

$$\mathcal{L} = -\log \frac{\exp(\text{sim}(h(\text{PS}(\tilde{X}, \tilde{A}, a_i)), h(\text{PS}(\tilde{X}, \tilde{A}, a_j))/\tau)}{\sum \exp(\text{sim}(h(\text{PS}(\tilde{X}, \tilde{A}, a_i)), h(\text{NS}(\tilde{X}, \tilde{A}, a_j))/\tau)} + ||\tilde{X} - \hat{X}||_2 \quad (5)$$

where \tilde{X} is the concatenated feature matrix of all pretraining datasets after projection (Equation 1), \tilde{A} is the adjacency matrix after being connected by the coordinators (Equation 2), PS, NS respectively denote the positive sampling and negative sampling, sim denotes a similarity metric (e.g., cosine similarity), a_i, a_j are different graph augmentations, and λ is the reconstruction loss coefficient that controls how much attention is paid to the reconstruction task.

3.4 Applying Knowledge to Downstream Data

Our pretraining methodology is inherently flexible and agnostic to downstream task constraints, making it compatible with various adaptation techniques. For instance, the recent introduction of prompting in the graph field has attracted considerable interest due to its remarkable efficiency and effectiveness [36]. To show the superior generalization ability of our GCOPE method, we explore its transferability within both the conventional finetuning paradigm and the nascent graph prompt framework.

Drawing inspiration from the methodology presented by [36], we cast downstream tasks into a graph-level framework. As delineated in their work, the maximal retention of pretraining knowledge is observed when downstream tasks are aligned within the same task space as the pretraining task. Given our pretraining is conducted at the graph level, we correspondingly transform all downstream tasks to this level by constructing induced subgraphs. The main algorithm is presented in Algorithm 1.

Algorithm 1: GCOPE

Table 1: Statistics of datasets.

Homophilic Data	Cora	Citeseer	Pubmed	Computers	Photos
# Nodes	2,708	3,327	19,717	13,752	7,650
# Edges	10,556	9,104	88,648	491,722	238,162
# Features	1,433	3,703	500	767	745
# Labels	7	6	3	10	8
h(G)	0.810	0.736	0.802	0.777	0.827
Heterophilic Data	Wisconsin	Texas	Cornell	Chameleon	Squirrel
# Nodes	251	183	183	2,277	5,201
# Edges	515	325	298	62792	396,846
# Features	1,703	1,703	1,703	2,325	2,089
# Labels	5	5	5	5	5
h(G)	0.196	0.108	0.305	0.231	0.222

3.5 Complexity Analysis

Thanks to the simplicity of our pretraining framework, the increase in parameter complexity is only marginal. The only additional parameters introduced are the features of the coordinators, with a complexity of $O(Md_{\rm A})$, which scales linearly with the number of pretraining datasets. In practical settings, scenarios characterized by an excessively abundant availability of pretraining datasets are rare. Assuming GNN we employ comprises L layers with a maximum layer width of d, and let $N = \sum_{k=1}^M |\mathcal{V}^{(k)}|$ and $E = \sum_{k=1}^M |\mathcal{E}^{(k)}|$. It is worth noting that the time complexity of a typical graph model, such as Graph Convolutional Network (GCN), is $O(LNd^2 + LEd + Nd)$ [36]. With the incorporation of coordinators, the revised time complexity becomes $O(L(N+M)d^2 + L(E+N+M)d + (N+M)d)$. The additional time complexity is $O(LMd^2 + L(N+M)d + Md)$. Given that $M \ll N$, the supplementary time cost scales nearly linearly with the number of original nodes.

4 EXPERIMENTS

In this section, we study the experimental results of our proposed method and baselines to answer five research questions:

- RQ1. What advantages does our proposed GCOPE method offer over representative baselines in cross-domain transfer learning?
- RQ2. How significant is the presence of edges among different coordinators?
- **RQ3.** Is the reconstruction loss necessary in GCOPE?
- RQ4. Can downstream prompts derive benefits from the crossdomain pretraining?
- **RQ5.** Which projection operation is more compatible for CCOPE?

4.1 Experimental Setup

Datasets. For comprehensive comparisons, we conduct experiments on ten real-world datasets. We choose five homophily datasets in experiments, including Cora [32], Citeseer [32], Pubmed [29], Computers and Photos datasets [28, 33], and five heterophilic datasets, including three sub-datasets derived from the WebKB [30] (Cornell, Texas, and Wisconsin) and two page-page networks (Chameleon and Squirrel) extracted from Wikipedia [30]. Table 1 summarizes the details, where h(G) is a metric that represents the degrees of homophily and heterophily. The values of h(G) are directly drawn from [45], indicating that the first five datasets are highly homophilic and the latter five are highly heterophilic [27, 45]. Different degrees of homophily and heterophily indicate different semantics in graphs. For more detailed information on these datasets, please check in Appendix.

Table 2: Cross-domain transfer learning performance (mean±std Acc/AUC/F1) on homophilic datasets (C-way-1-shot). IMP (%): the average improvement of GCOPE over the rest. GCL and Sim respectively represent GraphCL and SimGRACE.

Training schemes	Methods	Acc	Cora AUC	F1	Acc	Citeseer AUC	F1	Acc	Pubmed AUC	F1	Acc	Computers	F1	Acc	Photos AUC	F1
	GCN	0.3012±.06	0.6444±.04	0.2591±.04	0.4358±.09	0.7234±.07	0.3583±.10	0.4210±.01	0,6040±.06	0.3026±.04	0.2602±.07	0.6773±.02	0.2428±.04	0.4603±.04	0.8458±.01	0.4592±.04
	GAT	0.3646±.04	0.6769±.03	0.3108±.04	0.3695±.05	0.7232±.06	0.3305±.04	0.4210±.04	0.5710±.06	0.3227±.07	0.3482±.07	0.6878±.05	0.2397±.05	0.4742±.08	0.8213±.02	0.4498±.07
supervised	BWGNN	0.2543±.05	0.5563±.03	0.1971±.02	0.3599±.07	0.6954±.05	0.3112±.06	0.3976±.03	0.4934±.03	0.2686±.04	0.2768±.05	0.6273±.03	0.1864±.03	0.4113±.04	0.7769±.00	0.3883±.01
	FAGCN	0.3819±.03	0.6818±.04	0.3009±.09	0.5219±.08	0.8042±.03	$0.4667 \scriptstyle{\pm .08}$	0.4522±.02	$0.5622 \scriptstyle{\pm .04}$	$0.4275 \scriptstyle \pm .07$	0.4651±.04	0.7762±.02	0.3009±.07	0.5937±.05	0.8847±.00	$0.5346 \scriptstyle{\pm .03}$
	GCL+GCN	0.2507±.06	0.6350±.03	0.2240±.03	0.3140±.02	0.6661±.04	0.2397±.02	0.4217±.02	0.5257±.05	0.2896±.07	0.2856±.04	0.6467±.03	0.1653±.06	0.5533±.01	0.8661±.01	0.5217±.01
IP	GCL+FAGCN	0.3892±.05	0.7228±.03	$0.3619 \scriptstyle{\pm .05}$	0.4461±.02	0.7781±.01	$0.4126 \scriptstyle{\pm .02}$	0.4532±.02	0.5708±.03	0.4168±.04	0.4371±.06	0.7616±.01	$0.3450 \scriptstyle{\pm .02}$	0.6273±.01	$0.8710 \scriptstyle{\pm .01}$	$0.5406 \scriptstyle{\pm .03}$
+	Sim+GCN	0.2492±.02	$0.5765 \scriptstyle{\pm .03}$	$0.1567 \scriptstyle{\pm .04}$	0.2950±.06	$0.6203 \scriptstyle{\pm .06}$	$0.1812 \scriptstyle{\pm .06}$	0.3980±.01	$0.5067 \scriptstyle{\pm .02}$	$0.2805 \scriptstyle{\pm .01}$	0.2666±.10	$0.6286 \scriptstyle{\pm .01}$	$0.1603 \scriptstyle{\pm .03}$	0.4290±.04	$0.7645 \scriptstyle{\pm .02}$	$0.3955 \scriptstyle{\pm .02}$
finetuning	Sim+FAGCN	0.3957±.03	$0.7284 \scriptstyle{\pm .02}$	$0.3585 \scriptstyle{\pm .01}$	0.5101±.03	$0.7969 {\scriptstyle \pm .01}$	$0.4615 \scriptstyle{\pm .04}$	0.4398±.01	$0.5535 \scriptstyle{\pm .01}$	$0.4225 {\scriptstyle \pm .02}$	0.4393±.01	$0.7718 \scriptstyle{\pm .02}$	$0.3100 \scriptstyle{\pm .02}$	0.5704±.02	$0.8543 \scriptstyle \pm .02$	$0.4984 \scriptstyle{\pm .01}$
o coopp	GCL+GCN	0.3368±.02	0.6971±.04	0.2967±.03	0.3701±.03	0.7066±.02	0.3265±.05	0.4443±.04	0.5888±.04	0.4242±.04	0.3439±.03	0.7023±.01	0.2976±.03	0.5635±.02	0.8733±.00	0.5480±.02
GCOPE	GCL+FAGCN	0.4618±.03	0.7597±.05	$0.4388 \scriptstyle{\pm .05}$	0.5631±.03	$0.8258 \scriptstyle{\pm .02}$	$0.4953 \pm .04$	0.4591±.01	$0.5512 \scriptstyle \pm .01$	$0.4203 \pm .03$	0.4465±.01	$0.7747 \scriptstyle \pm .00$	$0.3432 \scriptstyle{\pm .03}$	0.6329±.02	0.8850±.00	$0.5935 \scriptstyle{\pm .03}$
+	Sim+GCN	0.2525±.05	0.5744±.03	$0.1722 {\scriptstyle \pm .06}$	0.3475±.05	$0.6527 \scriptstyle \pm .05$	$0.2704 \scriptstyle{\pm .05}$	0.4116±.00	$0.5166 \scriptstyle{\pm .04}$	$0.2994 \pm .03$	0.3230±.01	$0.6994 \pm .00$	$0.2515 \scriptstyle{\pm .00}$	0.4772±.03	$0.7851 \scriptstyle{\pm .01}$	$0.4277 \scriptstyle \pm .02$
finetuning	Sim+FAGCN	0.3875±.04	$0.7163{\scriptstyle \pm .03}$	$0.3355{\scriptstyle\pm.08}$	$0.5704 \scriptstyle{\pm .04}$	$0.8425 \scriptstyle{\pm .01}$	$0.5178 \scriptstyle{\pm .04}$	0.4727±.03	$0.5587 \scriptstyle \pm .03$	$0.5672 \scriptstyle \pm .03$	0.4677±.04	$0.7875 \scriptstyle \pm .01$	$0.3823 \scriptstyle{\pm .02}$	0.5985±.02	$0.8757 \scriptstyle \pm .02$	$0.5556 \scriptstyle{\pm .05}$
IM	1P (%)	11.23%	5.23%	14.63%	13.81%	4.26%	16.59%	5.02%	0.99%	25.32%	13.79%	6.28%	30.70%	10.31%	2.30%	12.18%

Table 3: Cross-domain transfer learning performance (mean±std Acc/AUC/F1) on heterophilic datasets (C-way-1-shot).

Training	Methods		Wisconsin			Texas			Cornell			Chameleon			Squirrel	
schemes		Acc	AUC	F1	Acc	AUC	F1	Acc	AUC	F1	Acc	AUC	F1	Acc	AUC	F1
	GCN	0.6290±.05	0.8320±.04	0.4871±.14	0.5812±.08	0.6731±.04	0.4557±.10	0.3263±.04	0.5666±.01	0.3151±.03	0.2393±.03	0.5310±.04	0.1923±.03	0.2093±.00	0.5263±.01	0.1889±.01
supervised	GAT	0.6009±.02	$0.8346 \scriptstyle{\pm .01}$	$0.5217 \scriptstyle \pm .05$	0.6300±.08	$0.5854 \scriptstyle{\pm .08}$	$0.4282 \pm .13$	0.3275±.14	$0.5306 \scriptstyle{\pm .03}$	$0.1497 \scriptstyle \pm .04$	0.2342±.02	$0.5205 \scriptstyle{\pm .04}$	$0.1379 \scriptstyle \pm .03$	0.2118±.00	$0.5195 \scriptstyle{\pm .02}$	$0.1160 \scriptstyle{\pm .01}$
superviseu	BWGNN	0.5620±.05	$0.8463 \scriptstyle{\pm .02}$	$0.5189 \scriptstyle \pm .05$	0.7438±.10	$0.6642 \pm .07$	$0.6274 \scriptstyle{\pm .22}$	0.3150±.09	$0.5938 \scriptstyle{\pm .06}$	$0.2190 \scriptstyle{\pm .05}$	0.2206±.02	$0.5039 \scriptstyle \pm .03$	$0.1540{\scriptstyle \pm .03}$	0.2155±.00	$0.5149 \scriptstyle \pm .00$	$0.1664 \scriptstyle{\pm .02}$
	FAGCN	0.5222±.05	$0.7905 \scriptstyle{\pm .0310}$	$0.4725{\scriptstyle \pm .06}$	0.6900±.06	$0.7185 \scriptstyle{\pm .01}$	$0.5334 \scriptstyle{\pm .12}$	0.2938±.06	$0.6573 \scriptstyle \pm .04$	$0.2872 \scriptstyle \pm .05$	0.2575±.02	$0.5515{\scriptstyle\pm.02}$	$0.1941 \scriptstyle \pm .01$	0.2181±.00	$0.5202 \scriptstyle{\pm .00}$	$0.1875 \scriptstyle{\pm .02}$
IP	GCL+GCN	0.5249±.03	0.7876±.03	0.4415±.05	0.7350±.01	0.7210±.02	0.5636±.09	0.4175±.04	0.6350±.02	0.3500±.04	0.2249±.02	0.5213±.00	0.1432±.03	0.2118±.01	$0.5059 \scriptstyle{\pm .01}$	0.1110±.03
ır	GCL+FAGCN	0.6063±.04	$0.8356 \pm .01$	$0.5555 {\scriptstyle \pm .07}$	0.7425±.03	$0.7034 \scriptstyle{\pm .03}$	$0.6141 {\scriptstyle \pm .09}$	0.2588±.04	$0.6262 \scriptstyle{\pm .04}$	$0.2442 \scriptstyle \pm .04$	0.2443±.00	$0.5530 \scriptstyle \pm .01$	$0.1875 \scriptstyle{\pm .01}$	0.2223±.00	$0.5307 \scriptstyle{\pm .00}$	$0.1740{\scriptstyle \pm .02}$
finetuning	Sim+GCN	0.5258±.04	$0.7927 \scriptstyle{\pm .05}$	$0.4604 \scriptstyle{\pm .06}$	0.6338±.05	$0.6024 \scriptstyle{\pm .07}$	$0.4269 \scriptstyle{\pm .14}$	0.3438±.13	$0.5954 \scriptstyle \pm .09$	0.2168±.09	0.2271±.01	$0.5183 \scriptstyle{\pm .02}$	0.1578±.03	0.2133±.00	$0.5133 \scriptstyle \pm .01$	$0.1550 \scriptstyle{\pm .02}$
inictuining	Sim+FAGCN	0.6335±.02	$0.8557 \scriptstyle \pm .00$	$0.5830 \scriptstyle{\pm .04}$	0.6725±.14	$0.6922 \scriptstyle{\pm .04}$	$0.5906 \pm .10$	0.2725±.05	$0.6433 \scriptstyle \pm .04$	$0.2617 \scriptstyle{\pm .04}$	0.2748±.01	$0.5652 \scriptstyle{\pm .00}$	$0.2011 {\scriptstyle \pm .00}$	0.2170±.00	$0.5213 \scriptstyle{\pm .00}$	$0.1716 \scriptstyle \pm .01$
GCOPE	GCL+GCN	0.6606±.04	0.8487±.01	0.5952±.04	0.7738±.06	0.7387±.01	0.6763±.08	0.3975±.10	0.6694±.04	0.3120±.04	0.2411±.01	0.5564±.00	0.2210±.00	0.2245±.00	0.5207±.01	0.1741±.00
GCOFE	GCL+FAGCN	0.6579±.03	$0.8531 \scriptstyle{\pm .01}$	$0.5649 \scriptstyle \pm .00$	0.7125±.02	$0.6693 \scriptstyle{\pm .02}$	$0.6300 \scriptstyle{\pm .03}$	0.4013±.05	$0.6897 \scriptstyle \pm .01$	$0.3160 \scriptstyle{\pm .02}$	0.2886±.00	$0.5898 \scriptstyle{\pm .00}$	$0.2320 \pm .00$	0.2257±.00	$0.5257 \scriptstyle{\pm .00}$	$0.1885 \scriptstyle{\pm .01}$
+	Sim+GCN	0.5412±.03	$0.8059 \scriptstyle{\pm .02}$	$0.4509 \scriptstyle{\pm .06}$	0.6137±.18	0.6900±.03	$0.4674 \scriptstyle{\pm .10}$	0.3675±.09	0.6045±.04	$0.2339 \pm .04$	0.2573±.02	$0.5467 \scriptstyle \pm .01$	$0.1852 \scriptstyle{\pm .01}$	0.2180±.00	$0.5147 \scriptstyle{\pm .00}$	$0.1783 \scriptstyle{\pm .00}$
finetuning	Sim+FAGCN	0.7321±.00	$0.9305 \scriptstyle{\pm .00}$	$0.6873 \scriptstyle \pm .01$	0.7950±.03	$0.7451 \scriptstyle \pm .01$	$0.7042 \scriptstyle{\pm .03}$	0.5925±.01	$0.8069 \scriptstyle{\pm .03}$	$0.4626 \scriptstyle{\pm .03}$	0.2894±.01	$0.5662 \scriptstyle{\pm .02}$	$0.2192 \scriptstyle{\pm .02}$	0.2193±.00	$0.5370 \scriptstyle \pm .00$	$0.1984 \scriptstyle{\pm .01}$
IM	1P (%)	12.57%	4.58%	13.76%	6.65%	6.08%	16.87%	37.66%	14.29%	29.62%	11.97%	6.01%	25.36%	3.25%	1.06%	16.39%

Baselines. We compare our proposed method with the following baselines, categorized into three groups and accompanied by concise descriptions. (1) Supervised methods: These methods train a GNN model on a downstream task and infer results directly. In this work, four famous GNN models are adopted, including GCN [16], GAT [40], BWGNN [38], and FAGCN [1]. We choose GCN and FAGCN as the backbones for our proposed GCOPE method since FAGCN is tailored to address both homophilic and heterophilic graphs [45] and GCN, a widely used GNN model, is the basis of FAGCN. (2) Isolated Pretraining (IP) with finetuning: These methods initially utilize multiple cross-domain datasets as source datasets, which are combined in an isolated manner to pretrain a GNN model in a self-supervised fashion (e.g. GraphCL [46] or SimGRACE [43]). Here, 'isolated' denotes that the datasets are amalgamated into a batch object without establishing inter-dataset connections, resulting in an adjacency matrix composed of distinct blocks. Subsequently, the pretrained model undergoes finetuning for a new downstream task. (3) Graph Coordinators for Pretraining (GCOPE) with transferring: With learnable coordinators, our proposed GCOPE method aims to unify the isolated source datasets into one large-scale dataset with inter-dataset connections for pretraining and then transfer the pretrained GNN model to a downstream task via finetuning or prompting [36].

Metrics and Implementations. We choose three widely used metrics to evaluate the node classification task [9, 13, 36, 45], including classification accuracy (Acc), mean AUC-ROC (AUC), and mean F1-score (F1). We leverage a 10-fold partition strategy to split the 10 real-world datasets, nine datasets as cross-domain source datasets for pretraining and the rest one dataset as the target dataset for transferring. To unify features of multiple cross-domain source datasets onto one single plane, we leverage SVD to reduce the initial features to 100 dimensions. We fix the number of graph neural layers at 2, with a hidden dimension of 100 for GCN, FAGCN, and GAT models. Additionally, we adopt the identical hyperparameters as specified in [38] for BWGNN. For all networks, we apply the Adam optimizer and the learning rate is assigned as 0.0001. In terms of GCOPE, we introduce one coordinator for each source dataset and assign 0.2 as the default reconstruction weight. Finally, in the transferring stage, we adopt node classification as the downstream task. For fair comparisons, we apply the C-way-K-shot learning setting, same as [26], for each target dataset to build the training data and then split the rest of the data randomly in 1:9 for validating and testing. In this paper, we report average results on all downstream tasks. More implementation details are shown in Appendix A, in which we also analyze the performance of GCOPE with more coordinators and dynamical edges between coordinators.

4.2 Cross-domain Transfer Performance with Few-shot Learning Settings (RQ1)

We compare our proposed GCOPE method with all the baselines on the downstream node classification tasks under the C-way-1-shot setting. We repeat the evaluation 5 times and report the average results and standard deviations in Table 2 and Table 3. The results of supervised methods are the benchmark to help validate whether the pretrained GNN models effectively transfer to the downstream tasks. As is known, pretraining GNNs aims to transfer prior knowledge from upstream tasks to improve the performance of GNNs on downstream tasks, especially in few-shot scenarios. However, we observe that most IP with finetuning methods struggle to achieve better performance compared with supervised methods, embodying the negative transfer phenomenon. This is due to the apparent differences in distribution across cross-domain datasets. Under the IP strategy, each graph sample only contains information from one of the nine distributions, making it challenging for GNN models to fit the nine independent distributions into a unified one and learn general graph representations effectively. In contrast, our proposed GCOPE with finetuning methods significantly outperforms almost all baselines, achieving positive transfer. This is because coordinators connect all the source datasets together, unifying nine independent distributions into one cohesive joint distribution. In the pretraining stage, all the training samples are drawn from this joint distribution, facilitating the sharing of information across cross-domain datasets. Consequently, the GNN model is able to balance the shared information and learn better graph representations for transferring knowledge on the downstream task. The reported improvements range from 3.25% up to 37.66% in terms of node classification accuracy. Kindly note that our few-shot experiment settings are different from the classic few-shot node classification settings that are actually designed for the meta-learning task. Additionally, we also evaluate our proposed GCOPE on C-way-3-shot and C-way-5-shot settings, shown in Table A1 and Table A2.

4.3 Interconnectivity Analysis (RQ2)

In this section, we investigate the impact of edges between different coordinators on the effectiveness of our proposed GCOPE framework. Specifically, we compare two variants: GCOPE/w, which includes inter-coordinator edges, and GCOPE/wo, which excludes them. Both variants share the same hyperparameters, with FAGCN as the backbone model and pretraining based on GraphCL. Additionally, the datasets utilized for pretraining and downstream tasks are partitioned using the 10-fold strategy. Table 4 presents the node classification accuracy (mean±std). Our experimental findings underscore the essential and effective role of inter-coordinator edges in GCOPE.

4.4 Reconstruction Analysis (RQ3)

We conduct a comparison of downstream node classification performance on Citeseer between our proposed GCOPE method with varying reconstruction loss coefficient values λ , and a supervised method to assess the efficacy of the reconstruction module. Specifically, FAGCN serves as the backbone model for both GCOPE and the supervised method. For GCOPE, GraphCL is utilized as the pretraining strategy. All other hyperparameters between GCOPE and the supervised method are maintained consistent. Figure 3 depicts the experimental results, focusing on Acc, AUC, and F1 metrics.

Table 4: Node classification accuracy (mean±std) of GCOPE/wo and GCOPE/w, which represent GCOPE without or with inter-coordinator edges respectively.

Homo Data	GCOPE/wo	GCOPE/w	Hetero Data	GCOPE/wo	GCOPE/w
Cora	0.3575±.02	0.4618±.03	Wisconsin	0.6335±.04	0.6579±.03
Citeseer	0.5062±.02	0.5631±.03	Texas	0.6863±.04	0.7125±.02
Pubmed	0.4108±.03	0.4591±.01	Cornell	0.3212±.03	0.4013±.05
Computers	0.4244±.01	0.4465±.01	Chameleon	0.2647±.01	0.2886±.00
Photos	0.6037±.03	0.6329±.02	Squirrel	0.2177±.00	0.2257±.00

Our experimental findings yield the following observations: First, GCOPE without reconstruction ($\lambda = 0.0$) outperforms the supervised pretraining, highlighting the effectiveness of the introduced coordinators. Second, GCOPE with reconstruction ($\lambda > 0.0$) achieves optimal performance when λ is set to 0.2, surpassing both the supervised pretraining and GCOPE ($\lambda = 0.0$). This improvement is attributed to the reconstruction module's ability to align graph features across datasets, facilitating more effective learning of shared information by GNNs from cross-domain source datasets. Third, as λ exceeds 0.2, performance begins to deteriorate, ultimately falling short of both the supervised pretraining and GCOPE ($\lambda = 0.0$). This decline can be attributed to excessively large λ values, which cause the model to overly prioritize reconstruction at the expense of its primary pretraining task. In summary, the inclusion of the reconstruction module with relatively small λ values proves essential for our proposed GCOPE method.

4.5 Transferring by Graph Prompt (RQ4)

In addition to finetuning, we explore the feasibility of leveraging the graph prompt technique to transfer upstream cross-domain knowledge learned by GCOPE. Specifically, we adopt the implementation of ProG [36], a widely used graph prompt method, which involves freezing the parameters of pretrained GNNs and incorporating graph prompts in the downstream node classification task. Subsequently, we evaluate the performance of GCOPE with ProG on four downstream datasets, comprising two homophilic and two heterophilic datasets. The experimental results are presented in Table 5. For comparison, we include results of the supervised method, IP with finetuning, and GCOPE with finetuning.

Based on our experimental observations, we draw the following conclusions: In comparison to the supervised and IP with finetuning methods, both GCOPE with finetuning and GCOPE with ProG exhibit superior performance. Notably, GCOPE with ProG achieves positive transfer with minimal tunable parameters in the downstream node classification task. While the performance of GCOPE with ProG is slightly lower than that of GCOPE with finetuning, the disparity between the two methods is significantly narrower than that between GCOPE with ProG and the supervised method. Based on the aforementioned analysis, we can assert that our proposed GCOPE framework can effectively benefit downstream prompts.

4.6 Compatibility Analysis of Projection Operation (RQ5)

To study the compatibility of various projection operations, we evaluate our proposed GCOPE method with SVD or attention mechanism across ten cross-domain real-world datasets. Specifically, we set FAGCN as the backbone, leverage GraphCL for pretraining, and finally transfer the pretrained GNNs to the downstream C-way

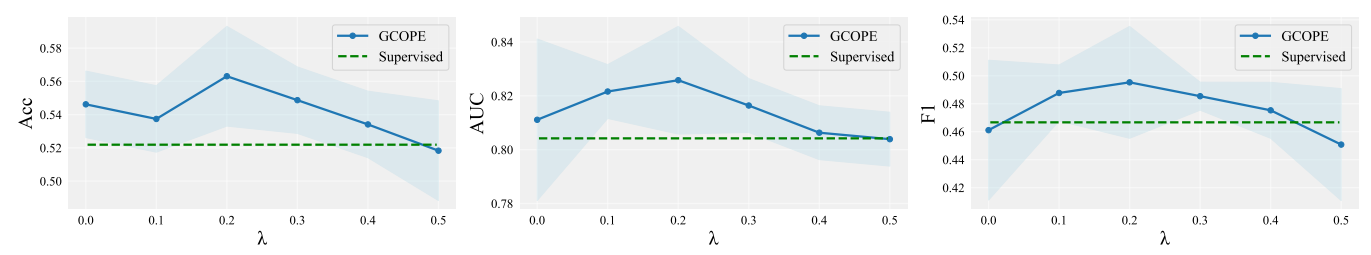


Figure 3: Node classification performance (mean±std) of GCOPE with varying reconstruction loss coefficient (λ) values on Citeseer under C-way-1-shot setting.

Table 5: Cross-domain transfer learning performance (mean±std Acc/AUC/F1) of GCOPE with ProG (C-way-1-shot). GCL and Sim respectively represent GraphCL and SimGRACE.

Training schemes	Methods	Acc	Cora AUC	F1	Acc	Citeseer AUC	F1	Acc	Wisconsin AUC	F1	Acc	Texas AUC	F1
supervised	FAGCN	0.3819±.03	0.6818±.04	0.3009±.09	0.5219±.08	0.8042±.03	0.4667±.08	0.5222±.03	0.7905±.03	0.4725±.06	0.6900±.06	0.7185±.01	0.5334±.01
IP + finetuning	GCL+FAGCN Sim+FAGCN		0.7228±.03 0.7284±.02	0.3619±.05 0.3858±.01						0.5555±.07 0.5830±.04		0.7034±.03 0.6922±.04	
GCOPE + ProG	GCL+FAGCN Sim+FAGCN	0.4283±.03 0.3941±.01	0.7552±.01 0.6892±.03	0.4326±.01 0.3507±.09						$0.6359 \scriptstyle{\pm .07} \\ 0.6579 \scriptstyle{\pm .01}$		$0.6689 \scriptstyle{\pm .00} \\ 0.7356 \scriptstyle{\pm .01}$	
GCOPE + finetuning	GCL+FAGCN Sim+FAGCN	0.4618±.03 0.3875±.04	0.7597±.05 0.7163±.03	0.4388±.05 0.3355±.08					0.8531±.01 0.9305±.00	0.5649±.00 0.6873±.01		0.6693±.02 0.7451±.01	0.6300±.03 0.7042±.03

Table 6: Accuracy (mean±std) of GCOPE with finetuning on different projection operations. Experiment settings are the same as Table 2.

Homo Data	Attention	SVD	Hetero Data	Attention	SVD
Cora	0.3120±.02	0.4618±.03	Wisconsin	0.5692±.05	0.6579±.03
Citeseer	0.3861±.07	0.5631±.03	Texas	0.6663±.06	0.7125±.02
Pubmed	0.4475±.02	0.4591±.01	Cornell	0.3737±.03	0.4013±.05
Computers	0.3689±.06	0.4465±.01	Chameleon	0.2755±.00	0.2886±.00
Photos	0.4857±.04	0.6329±.02	Squirrel	0.2210±.00	0.2257±.00

1-shot node classification tasks. For GCOPE with attention mechanism, we equip each dataset with a data-specific attention module to project their respective features into a shared plane, regardless of their position in the pretraining and finetuning pipeline. We report the node classification accuracy (mean±std) in Table 6. We can easily observe that GCOPE with attention mechanism significantly underperforms the ones with SVD. This could be attributed to the fact that the utilized samples are insufficient to train attention modules effectively. Each attention module has 32, 792, 288 tuned parameters, while SVD is a non-parametric mathematical method. Therefore, we ensure that SVD is more compatible under few-shot learning scenarios. For effectiveness and simplicity, we set SVD as the default projection operation of GCOPE in this work.

5 RELATED WORK

Graph Pretraining. In the machine learning (ML) research field, pretraining is widely acknowledged for its ability to leverage existing data to train a feature extractor with robust generalization capabilities [5, 21, 24, 31, 50]. Specifically within the graph domain, pretraining methods can be categorized into three main types: generation-based, auxiliary property-based, and contrast-based methods [25]. Generation-based methods utilize feature or

structure reconstruction as the loss function to extract embeddings with strong generalization properties (*e.g.*, GAE [15], Graph-MAE [12], and GraphMAE2 [11]). Auxiliary property-based methods introduce new attributive or structural properties as supervision signals, such as clustering pseudo labels utilized by M3S [35]. Contrast-based methods define positive and negative embedding pairs and aim to bring positive pairs closer while pushing negative pairs apart. Among these three categories, contrast-based methods have garnered the most popularity and achieved notable successes [8, 10, 34, 41, 43, 46, 51]. However, despite the success of these methods across various graph tasks, none have managed to achieve the objective of pretraining on multiple graph datasets belonging to different domains. Consequently, the efficacy of pretraining remains constrained by the size and diversity of the source data. This remains an open question in the graph pretraining field.

Graph Transfer Learning. Recent years have witnessed significant advancements in GNNs. However, adapting pre-trained GNNs to diverse downstream tasks efficiently remains a challenge. Traditionally, finetuning, as presented in [3, 17, 52], has dominated this field. This approach leverages a pretrained GNN as a foundation, finetuning either the final layer or the entire model for the specific task. Finetuning has consistently achieved state-of-the-art (SOTA) performance.

However, recent exploration has led to the emergence of graph prompts [18, 36, 37, 42] as a compelling alternative, drawing inspiration from the NLP community's 'prompting' paradigm [19, 23, 44]. As detailed in [36], a graph prompt comprises three key elements: prompt tokens, which contain the prompt content in the form of vectors; token structures, which depicts how the tokens are connected; inserting patterns, which fuses the graph prompt with the target data. By carefully crafting these components, often through learning-based approaches, graph prompts can effectively transfer

knowledge from the pretrained model to new tasks. While not guaranteed to outperform finetuning in every scenario, graph prompts excel in terms of efficiency due to their minimal parameter footprint. This shift towards graph prompts highlights the ongoing exploration of efficient and effective knowledge transfer within the realm of GNNs. Further research is warranted to refine prompt construction strategies and assess their broader applicability across diverse downstream tasks.

6 CONCLUSION

This study delves into the intricate phenomenon of negative transfer within the field of graph learning, shedding light on its complexities through a rigorous analysis. In response, we introduce an innovative pretraining approach named GCOPE, devised to effectively mitigate negative transfer effects. GCOPE leverages coordinators to seamlessly amalgamate disparate graphs, establishing interconnections and aligning their features. Our thorough experimentation, conducted across a spectrum of homophilic and heterophilic datasets, vividly demonstrates the efficacy of our proposed method.

Despite the notable success achieved by GCOPE, it is prudent to acknowledge the potential limitations stemming from the non-parametric nature of SVD. This aspect may constrain the method's generalizability across diverse datasets. As such, our future research endeavors will be directed towards devising a more robust learning-based feature projection pipeline, which naturally understands and aligns features of graphs from a variety of domains.

ACKNOWLEDGMENTS

This Research of Li was supported by NSFC Grant No. 62206067 and Guangzhou-HKUST(GZ) Joint Funding Scheme 2023A03J0673. The research of Cheng was supported in part by project #MMT-p2-23 of the Shun Hing Institute of Advanced Engineering, The Chinese University of Hong Kong and by grants from the Research Grant Council of the Hong Kong Special Administrative Region, China (No. CUHK 14217622).

REFERENCES

- Deyu Bo, Xiao Wang, Chuan Shi, and Huawei Shen. 2021. Beyond low-frequency information in graph convolutional networks. In Proceedings of the AAAI Conference on Artificial Intelligence, Vol. 35. 3950–3957.
- [2] Aochuan Chen, Yuguang Yao, Pin-Yu Chen, Yihua Zhang, and Sijia Liu. 2023. Understanding and improving visual prompting: A label-mapping perspective. In Proceedings of the IEEE/CVF Conference on Computer Vision and Pattern Recognition. 19133–19143.
- [3] Nuo Chen, Yuhan Li, Jianheng Tang, and Jia Li. 2024. GraphWiz: An Instruction-Following Language Model for Graph Problems. arXiv preprint arXiv:2402.16029 (2024).
- [4] Ting Chen, Simon Kornblith, Mohammad Norouzi, and Geoffrey Hinton. 2020. A simple framework for contrastive learning of visual representations. In *Interna*tional conference on machine learning. PMLR, 1597–1607.
- [5] Jacob Devlin, Ming-Wei Chang, Kenton Lee, and Kristina Toutanova. 2018. Bert: Pre-training of deep bidirectional transformers for language understanding. arXiv preprint arXiv:1810.04805 (2018).
- [6] Zhengxiao Du, Yujie Qian, Xiao Liu, Ming Ding, Jiezhong Qiu, Zhilin Yang, and Jie Tang. 2021. All nlp tasks are generation tasks: A general pretraining framework.
- [7] Taoran Fang, Yunchao Zhang, Yang Yang, and Chunping Wang. 2022. Prompt tuning for graph neural networks. arXiv preprint arXiv:2209.15240 (2022).
- [8] Jean-Bastien Grill, Florian Strub, Florent Altché, Corentin Tallec, Pierre Richemond, Elena Buchatskaya, Carl Doersch, Bernardo Avila Pires, Zhaohan Guo, Mohammad Gheshlaghi Azar, et al. 2020. Bootstrap your own latent-a new approach to self-supervised learning. Advances in neural information processing systems 33 (2020), 21271–21284.
- [9] Russell Alan Hart, Linlin Yu, Yifei Lou, and Feng Chen. 2023. Improvements on Uncertainty Quantification for Node Classification via Distance Based Regularization. In Thirty-seventh Conference on Neural Information Processing Systems.

- [10] Kaveh Hassani and Amir Hosein Khasahmadi. 2020. Contrastive multi-view representation learning on graphs. In *International conference on machine learning*. PMLR. 4116–4126.
- [11] Zhenyu Hou, Yufei He, Yukuo Cen, Xiao Liu, Yuxiao Dong, Evgeny Kharlamov, and Jie Tang. 2023. GraphMAE2: A Decoding-Enhanced Masked Self-Supervised Graph Learner. In Proceedings of the ACM Web Conference 2023. 737–746.
- [12] Zhenyu Hou, Xiao Liu, Yukuo Cen, Yuxiao Dong, Hongxia Yang, Chunjie Wang, and Jie Tang. 2022. Graphmae: Self-supervised masked graph autoencoders. In Proceedings of the 28th ACM SIGKDD Conference on Knowledge Discovery and Data Mining. 594–604.
- [13] Jongwon Jeong, Hoyeop Lee, Hyui Geon Yoon, Beomyoung Lee, Junhee Heo, Geonsoo Kim, and Jin Seon Kim. 2024. iGraphMix: Input Graph Mixup Method for Node Classification. In *The Twelfth International Conference on Learning Representations*. https://openreview.net/forum?id=a2ljjXeDcE
- [14] Wei Jin, Tyler Derr, Haochen Liu, Yiqi Wang, Suhang Wang, Zitao Liu, and Jiliang Tang. 2020. Self-supervised learning on graphs: Deep insights and new direction. arXiv preprint arXiv:2006.10141 (2020).
- [15] Thomas N Kipf and Max Welling. 2016. Variational graph auto-encoders. arXiv preprint arXiv:1611.07308 (2016).
- [16] Thomas N. Kipf and Max Welling. 2017. Semi-Supervised Classification with Graph Convolutional Networks. In International Conference on Learning Representations.
- [17] Jaekoo Lee, Hyunjae Kim, Jongsun Lee, and Sungroh Yoon. 2017. Transfer learning for deep learning on graph-structured data. In Proceedings of the AAAI Conference on Artificial Intelligence, Vol. 31.
- [18] Yuhan Li, Zhixun Li, Peisong Wang, Jia Li, Xiangguo Sun, Hong Cheng, and Jeffrey Xu Yu. 2023. A survey of graph meets large language model: Progress and future directions. arXiv preprint arXiv:2311.12399 (2023).
- [19] Yuhan Li, Wei Shen, Jianbo Gao, and Yadong Wang. 2022. Community question answering entity linking via leveraging auxiliary data. arXiv preprint arXiv:2205.11917 (2022).
- [20] Yuhan Li, Peisong Wang, Zhixun Li, Jeffrey Xu Yu, and Jia Li. 2024. ZeroG: Investigating Cross-dataset Zero-shot Transferability in Graphs. arXiv preprint arXiv:2402.11235 (2024).
- [21] Yuhan Li, Jian Wu, Zhiwei Yu, Börje F Karlsso, Wei Shen, Manabu Okumura, and Chin-Yew Lin. 2023. Unlocking Science: Novel Dataset and Benchmark for Cross-Modality Scientific Information Extraction. arXiv preprint arXiv:2311.08189 (2023).
- [22] Hao Liu, Jiarui Feng, Lecheng Kong, Ningyue Liang, Dacheng Tao, Yixin Chen, and Muhan Zhang. 2023. One for all: Towards training one graph model for all classification tasks. arXiv preprint arXiv:2310.00149 (2023).
- [23] Pengfei Liu, Weizhe Yuan, Jinlan Fu, Zhengbao Jiang, Hiroaki Hayashi, and Graham Neubig. 2023. Pre-train, prompt, and predict: A systematic survey of prompting methods in natural language processing. *Comput. Surveys* 55, 9 (2023), 1–35.
- [24] Yang Liu, Jiashun Cheng, Haihong Zhao, Tingyang Xu, Peilin Zhao, Fugee Tsung, Jia Li, and Yu Rong. 2024. SEGNO: Generalizing Equivariant Graph Neural Networks with Physical Inductive Biases. In The Twelfth International Conference on Learning Representations. https://openreview.net/forum?id=3oTPsORaDH
- [25] Yixin Liu, Ming Jin, Shirui Pan, Chuan Zhou, Yu Zheng, Feng Xia, and S Yu Philip. 2022. Graph self-supervised learning: A survey. IEEE Transactions on Knowledge and Data Engineering 35, 6 (2022), 5879–5900.
- [26] Zemin Liu, Xingtong Yu, Yuan Fang, and Xinming Zhang. 2023. Graphprompt: Unifying pre-training and downstream tasks for graph neural networks. In Proceedings of the ACM Web Conference 2023. 417–428.
- [27] Sitao Luan, Chenqing Hua, Minkai Xu, Qincheng Lu, Jiaqi Zhu, Xiao-Wen Chang, Jie Fu, Jure Leskovec, and Doina Precup. 2023. When Do Graph Neural Networks Help with Node Classification? Investigating the Homophily Principle on Node Distinguishability. In Thirty-seventh Conference on Neural Information Processing Systems. https://openreview.net/forum?id=kJmYu3Ti2z
- [28] Julian McAuley, Christopher Targett, Qinfeng Shi, and Anton Van Den Hengel. 2015. Image-based recommendations on styles and substitutes. In Proceedings of the 38th international ACM SIGIR conference on research and development in information retrieval. 43–52.
- [29] Galileo Namata, Ben London, Lise Getoor, Bert Huang, and U Edu. 2012. Query-driven active surveying for collective classification. In 10th international workshop on mining and learning with graphs, Vol. 8. 1.
- [30] Hongbin Pei, Bingzhe Wei, Kevin Chen-Chuan Chang, Yu Lei, and Bo Yang. 2019. Geom-GCN: Geometric Graph Convolutional Networks. In International Conference on Learning Representations.
- [31] Tal Ridnik, Emanuel Ben-Baruch, Asaf Noy, and Lihi Zelnik-Manor. 2021. Imagenet-21k pretraining for the masses. arXiv preprint arXiv:2104.10972 (2021).
- [32] Prithviraj Sen, Galileo Namata, Mustafa Bilgic, Lise Getoor, Brian Galligher, and Tina Eliassi-Rad. 2008. Collective classification in network data. AI magazine 29, 3 (2008), 93–93.
- [33] Oleksandr Shchur, Maximilian Mumme, Aleksandar Bojchevski, and Stephan Günnemann. 2018. Pitfalls of graph neural network evaluation. arXiv preprint arXiv:1811.05868 (2018).

- [34] Fan-Yun Sun, Jordan Hoffmann, Vikas Verma, and Jian Tang. 2019. Infograph: Unsupervised and semi-supervised graph-level representation learning via mutual information maximization. arXiv preprint arXiv:1908.01000 (2019).
- [35] Ke Sun, Zhouchen Lin, and Zhanxing Zhu. 2020. Multi-stage self-supervised learning for graph convolutional networks on graphs with few labeled nodes. In Proceedings of the AAAI conference on artificial intelligence, Vol. 34. 5892–5899.
- [36] Xiangguo Sun, Hong Cheng, Jia Li, Bo Liu, and Jihong Guan. 2023. All in One: Multi-Task Prompting for Graph Neural Networks. In Proceedings of the 26th ACM SIGKDD international conference on knowledge discovery & data mining (KDD '23), 2120–2131.
- [37] Xiangguo Sun, Jiawen Zhang, Xixi Wu, Hong Cheng, Yun Xiong, and Jia Li. 2023. Graph Prompt Learning: A Comprehensive Survey and Beyond. arXiv preprint arXiv:2311.16534 (2023).
- [38] Jianheng Tang, Jiajin Li, Ziqi Gao, and Jia Li. 2022. Rethinking graph neural networks for anomaly detection. In *International Conference on Machine Learning*. PMLR, 21076–21089.
- [39] Hugo Touvron, Thibaut Lavril, Gautier Izacard, Xavier Martinet, Marie-Anne Lachaux, Timothée Lacroix, Baptiste Rozière, Naman Goyal, Eric Hambro, Faisal Azhar, et al. 2023. Llama: Open and efficient foundation language models. arXiv preprint arXiv:2302.13971 (2023).
- [40] Petar Veličković, Guillem Cucurull, Arantxa Casanova, Adriana Romero, Pietro Liò, and Yoshua Bengio. 2018. Graph Attention Networks. In International Conference on Learning Representations.
- [41] Petar Veličković, William Fedus, William L Hamilton, Pietro Liò, Yoshua Bengio, and R Devon Hjelm. 2018. Deep graph infomax. arXiv preprint arXiv:1809.10341 (2018).
- [42] Xuansheng Wu, Kaixiong Zhou, Mingchen Sun, Xin Wang, and Ninghao Liu. 2023. A survey of graph prompting methods: techniques, applications, and challenges. arXiv preprint arXiv:2303.07275 (2023).
- [43] Jun Xia, Lirong Wu, Jintao Chen, Bozhen Hu, and Stan Z Li. 2022. Simgrace: A simple framework for graph contrastive learning without data augmentation. In Proceedings of the ACM Web Conference 2022. 1070–1079.
- [44] Siheng Xiong, Ali Payani, Ramana Kompella, and Faramarz Fekri. 2024. Large language models can learn temporal reasoning. arXiv preprint arXiv:2401.06853 (2024).
- [45] Zhe Xu, Yuzhong Chen, Qinghai Zhou, Yuhang Wu, Menghai Pan, Hao Yang, and Hanghang Tong. 2023. Node classification beyond homophily: Towards a general solution. In Proceedings of the 29th ACM SIGKDD Conference on Knowledge Discovery and Data Mining. 2862–2873.
- [46] Yuning You, Tianlong Chen, Yongduo Sui, Ting Chen, Zhangyang Wang, and Yang Shen. 2020. Graph contrastive learning with augmentations. Advances in neural information processing systems 33 (2020), 5812–5823.
- [47] Wen Zhang, Lingfei Deng, Lei Zhang, and Dongrui Wu. 2022. A survey on negative transfer. IEEE/CAA Journal of Automatica Sinica 10, 2 (2022), 305–329.
- [48] Yihua Zhang, Yimeng Zhang, Aochuan Chen, Jinghan Jia, Jiancheng Liu, Gaowen Liu, Mingyi Hong, Shiyu Chang, and Sijia Liu. 2023. Selectivity Drives Productivity: Efficient Dataset Pruning for Enhanced Transfer Learning. arXiv preprint arXiv:2310.08782 (2023).
- [49] Haihong Zhao, Bo Yang, Jiaxu Cui, Qianli Xing, Jiaxing Shen, Fujin Zhu, and Jiannong Cao. 2023. Effective fault scenario identification for communication networks via knowledge-enhanced graph neural networks. *IEEE Transactions on Mobile Computing* (2023).
- [50] Haihong Zhao, Chenyi Zi, Yang Liu, Chen Zhang, Yan Zhou, and Jia Li. 2024. Weakly Supervised Anomaly Detection via Knowledge-Data Alignment. In Proceedings of the ACM on Web Conference 2024. 4083–4094.
- [51] Yun Zhu, Jianhao Guo, Fei Wu, and Siliang Tang. 2022. Rosa: a robust self-aligned framework for node-node graph contrastive learning. arXiv preprint arXiv:2204.13846 (2022).
- [52] Fuzhen Zhuang, Zhiyuan Qi, Keyu Duan, Dongbo Xi, Yongchun Zhu, Hengshu Zhu, Hui Xiong, and Qing He. 2020. A comprehensive survey on transfer learning. Proc. IEEE 109, 1 (2020), 43–76.

A APPENDIX

A.1 Codes and Datasets

Code available at https://github.com/cshhzhao/GCOPE. A more detailed information on related datasets is as follows:

• Citation network: Cora and Citeseer datasets [32] consist of a diverse collection of computer science publications, where each node is characterized by a bag-of-words representation of papers and a categorical label indicating the paper topic. Pubmed dataset [29] comprises articles related to diabetes from the PubMed database. Each node in this dataset is represented by an attribute

- vector containing TF/IDF-weighted word frequencies, accompanied by a label specifying the particular type of diabetes discussed in the publication.
- Amazon network: Computers and Photos datasets [28, 33] are
 two networks illustrating co-purchase relationships sourced from
 Amazon. In these networks, each node represents a product, and
 an edge indicates frequent co-purchases between two products.
 Additionally, each node is associated with a bag-of-words representation of product reviews and is labeled with its respective
 category.
- WebKB: Cornell, Texas, and Wisconsin are three subdatasets derived from the WebKB dataset [30], compiled from multiple universities' web pages. Each node within these datasets represents a web page, with edges denoting hyperlinks between pages. The node features are represented as bag-of-words representations of the web pages. Additionally, the web pages are manually categorized into five distinct labels: student, project, course, staff, and faculty.
- Wikipedia network: Chameleon and Squirrel datasets [30] consist of two page-page networks extracted from Wikipedia, focusing on specific topics. In these networks, nodes represent individual web pages, while edges signify links between pages. Node attributes are defined as sets of informative nouns extracted from the pages. Moreover, each node is labeled based on the average monthly traffic received by the respective web page.

A.2 Parameter Analysis

We compare parameter numbers of two baselines and our proposed GCOPE in Table A8. For downstream tasks, we also compare parameter numbers of finetuning and prompting in Table A8.

Table A8: Parameter analysis various methods, where the backbone is FAGCN. IP and GCOPE are pretrained by GraphCL. Citeseer is the downstream dataset. We use "-" to represent the case without corresponding phases.

Methods	Supervised	IP	GCOPE
Pretraining	-	62,976	62,976
+ Coordinators	-	-	900
+ Reconstruction	-	-	29,412
Finetuning	47,750	47,750	47,750
Prompting	-	-	19,398

A.3 Cross-domain Transfer Performance with other C-way-K-shot settings

We use Table A1, Table A2, Table A3, and Table A4 to show the cross-domain transfer learning performance with 3/5-shot learning scenarios respectively. From the experimental results, we observe that our proposed GCOPE maintains its superiority over other baseline methods, even though the improvements modestly decrease from 1-shot to 5-shot scenarios.

A.4 Quantitative Analysis of Graph Coordinators

We conduct additional experiments to investigate the quantitative analysis of graph coordinators, shown by Table A5 and Table A6. Experimental results show that, despite slight fluctuations in performance across different datasets, GCOPE with varying numbers of graph coordinators generally outperforms both the Supervised and IP methods.

Table A1: Cross-domain transfer learning performance (mean±std Acc/AUC/F1) on homophilic datasets (C-way 3-shot). IMP (%): the average improvement of GCOPE over the rest. GCL and Sim respectively represent GraphCL and SimGRACE.

Training	Methods		Cora			Citeseer			Pubmed			Computers			Photos	
schemes		Acc	AUC	F1	Acc	AUC	F1	Acc	AUC	F1	Acc	AUC	F1	Acc	AUC	F1
	GCN	0.4493±.05	0.7911±.02	$0.4425{\scriptstyle \pm .04}$	0.4336±.05	$0.7580 \scriptstyle{\pm .04}$	0.4131±.04	0.5565±.06	0.7161±.05	0.5343±.06	0.4516±.04	$0.7973 \scriptstyle{\pm .01}$	$0.4101 \scriptstyle{\pm .02}$	0.5816±.04	0.8786±.01	$0.5261 \scriptstyle{\pm .05}$
supervised	GAT	0.4741±.01	$0.8035 \scriptstyle{\pm .01}$	$0.4420 {\scriptstyle \pm .01}$	0.4813±.02	$0.7634 \scriptstyle{\pm .01}$	$0.4470 \scriptstyle \pm .02$	0.6250±.01	$0.7803 \scriptstyle{\pm .02}$	$0.5877 \scriptstyle \pm .04$	0.4077±.07	$0.7951 \scriptstyle{\pm .03}$	$0.3865 \scriptstyle{\pm .02}$	0.5935±.04	$0.8789_{\pm .02}$	$0.5595 \scriptstyle{\pm .05}$
superviseu	BWGNN	0.4887±.01	$0.8137 \scriptstyle \pm .01$	$0.4737 \scriptstyle \pm .01$	0.3840±.05	$0.7176 \scriptstyle \pm .03$	$0.3608 \scriptstyle{\pm .05}$	0.5423±.03	$0.6940 \scriptstyle{\pm .02}$	$0.5171 {\scriptstyle \pm .03}$	0.4554±.04	$0.8022 \scriptstyle{\pm .01}$	$0.4132 \scriptstyle{\pm .06}$	0.5749±.03	$0.8670 \scriptstyle{\pm .00}$	$0.5308 \scriptstyle{\pm .01}$
	FAGCN	0.6517±.01	0.8926±.00	$0.6336 \scriptstyle{\pm .01}$	0.6217±.02	$0.8416 \scriptstyle{\pm .00}$	$0.5888 \scriptstyle{\pm .02}$	0.5695±.03	$0.6267 \scriptstyle \pm .04$	$0.5201 \scriptstyle{\pm .02}$	0.5588±.06	$0.8695 \scriptstyle{\pm .02}$	$0.5300{\scriptstyle \pm .04}$	0.6582±.02	$0.9123 \scriptstyle{\pm .00}$	0.6431±.01
IP	GCL+GCN	0.4414±.06	0.7540±.03	0.4155±.04	0.4099±.04	0.7270±.04	0.3836±.07	0.5565±.03	0.7374±.01	0.5334±.02	0.4363±.03	0.8222±.01	0.4470±.01	0.5918±.04	0.8949±.01	0.5868±.03
+	GCL+FAGCN	0.6252±.02	$0.8945 \scriptstyle \pm .00$	$0.6129 \scriptstyle{\pm .02}$	0.6099±.02	$0.8469 \scriptstyle \pm .00$	$0.5767 \scriptstyle{\pm .02}$	0.5374±.02	$0.6134 \scriptstyle{\pm .02}$	$0.4643 \scriptstyle \pm .04$	0.5300±.06	$0.8799 {\scriptstyle \pm .00}$	$0.5226 \scriptstyle{\pm .03}$	0.6925±.02	$0.9247 \scriptstyle \pm .00$	$0.6575 \scriptstyle \pm .01$
finetuning	Sim+GCN	0.4290±.02	$0.7565 \scriptstyle{\pm .02}$	$0.3911 \pm .02$	0.3816±.05	$0.6938 \scriptstyle{\pm .04}$	$0.3375 \scriptstyle \pm .08$	0.5458±.04	$0.7008 \scriptstyle{\pm .02}$	$0.5083 \scriptstyle{\pm .04}$	0.4674±.02	$0.8057 \scriptstyle{\pm .02}$	$0.4061 \scriptstyle{\pm .07}$	0.5561±.03	$0.8525 \scriptstyle{\pm .01}$	$0.5131 \scriptstyle{\pm .03}$
imetuning	Sim+FAGCN	0.6758±.02	$0.9004 \pm .01$	$0.6467 \scriptstyle{\pm .02}$	0.5333±.02	$0.8064 \scriptstyle{\pm .00}$	$0.4992 {\scriptstyle \pm .02}$	0.5696±.02	$0.6201 \scriptstyle{\pm .03}$	$0.5031 \scriptstyle{\pm .05}$	0.5164±.03	$0.8531 \scriptstyle{\pm .01}$	$0.5111 {\scriptstyle \pm .02}$	0.6532±.01	$0.9301 \scriptstyle{\pm .00}$	$0.6482 \scriptstyle{\pm .01}$
GCOPE	GCL+GCN	0.4327±.03	0.7560±.04	0.4131±.03	0.4273±.02	0.7392±.02	0.3871±.03	0.5681±.02	0.7314±.01	0.5103±.05	0.4808±.02	0.8357±.01	0.4424±.04	0.6266±.02	0.8909±.01	0.5754±.03
GCOPE	GCL+FAGCN	0.6857±.02	$0.9166 \scriptstyle{\pm .00}$	$0.6721 \pm .02$	0.6148±.02	$0.8431 \scriptstyle \pm .01$	$0.5752 \scriptstyle \pm .02$	0.5490±.02	$0.6636 \scriptstyle{\pm .01}$	$0.4878 \scriptstyle{\pm .06}$	0.5493±.03	$0.8682 \scriptstyle{\pm .01}$	$0.5269 \scriptstyle{\pm .05}$	0.6873±.03	$0.9172 \scriptstyle \pm .01$	$0.6556 \scriptstyle{\pm .01}$
+ 6ti	Sim+GCN	0.4187±.01	0.7648±.03	$0.3841 \scriptstyle{\pm .05}$	0.4301±.00	$0.7212 \scriptstyle{\pm .00}$	$0.3952 \pm .03$	0.5606±.05	$0.7418 \scriptstyle{\pm .04}$	0.5246±.06	0.4432±.03	$0.7990 \scriptstyle{\pm .01}$	0.3968±.04	0.5890±.01	$0.8841 \scriptstyle{\pm .01}$	$0.5441 \scriptstyle \pm .03$
finetuning	Sim+FAGCN	0.6798±.04	$0.9010 \scriptstyle{\pm .02}$	$0.6617 \scriptstyle \pm .04$	0.6469±.02	0.8602±.00	$0.6120 \scriptstyle{\pm .02}$	0.6048±.03	$0.7081 \scriptstyle{\pm .07}$	0.5700±.05	0.5742±.02	$0.8684 \scriptstyle{\pm .01}$	$0.5480{\scriptstyle \pm .00}$	0.6938±.01	$0.9343{\scriptstyle \pm .00}$	0.6683±.00
IN	1P (%)	4.69%	1.07%	5.03%	9.93%	2.81%	9.21%	1.39%	3.66%	0.41%	7.10%	1.78%	5.56%	5.95%	1.60%	5.18%

Table A2: Cross-domain transfer learning performance (mean±std Acc/AUC/F1) on heterophilic datasets (C-way-3-shot). IMP (%): the average improvement of GCOPE over the rest. GCL and Sim respectively represent GraphCL and SimGRACE.

Training	M (1 1		Wisconsin			Texas			Cornell			Chameleon			Squirrel	
schemes	Methods	Acc	AUC	F1	Acc	AUC	F1									
	GCN	0.6642±.05	0.8406±.02	0.6136±.05	0.7085±.03	0.6826±.01	0.5778±.08	0.5444±.12	$0.8084 \pm .05$	0.5276±.06	0.2340±.02	$0.5359 \scriptstyle \pm .03$	0.1566±.05	0.2161±.00	$0.5228 \scriptstyle{\pm .00}$	$0.1916 \scriptstyle{\pm .01}$
supervised	GAT	0.5783±.05	$0.7976 \scriptstyle{\pm .02}$	$0.4903 \scriptstyle{\pm .05}$	0.6732±.04	$0.6320 \scriptstyle{\pm .03}$	$0.5533 \scriptstyle \pm .02$	0.4411±.11	$0.7879 \scriptstyle \pm .06$	$0.4410 {\scriptstyle \pm .07}$	0.2400±.01	$0.5401 \scriptstyle{\pm .01}$	$0.1782 \scriptstyle{\pm .04}$	0.2011±.01	$0.5064 \scriptstyle{\pm .01}$	0.1536±.03
super viseu	BWGNN	0.5868±.05	0.8212±.06	0.4435±.09	0.6654±.09	$0.6694 \scriptstyle{\pm .05}$	$0.4401 \scriptstyle{\pm .24}$	0.5417±.05	$0.7871 \scriptstyle \pm .07$	$0.4799 \scriptstyle \pm .05$	0.2245±.04	$0.4953 \scriptstyle{\pm .02}$	$0.1816 \scriptstyle{\pm .02}$	0.2096±.00	$0.5075 \scriptstyle{\pm .01}$	$0.1635 \scriptstyle{\pm .02}$
	FAGCN	0.7104±.01	$0.8655 \scriptstyle{\pm .01}$	$0.5972 \scriptstyle{\pm .02}$	0.7163±.04	$0.6728 \scriptstyle{\pm .01}$	$0.6105 \scriptstyle{\pm .04}$	0.5722±.10	$0.8638 \scriptstyle{\pm .02}$	$0.5835 \scriptstyle{\pm .09}$	0.2564±.02	$0.5425{\scriptstyle \pm .02}$	$0.2042 \scriptstyle{\pm .02}$	0.2053±.01	$0.5064 \scriptstyle{\pm .01}$	$0.1738 \scriptstyle{\pm .01}$
IP	GCL+GCN	0.5840±.07	0.8030±.08	0.4231±.19	0.6510±.08	0.6508±.02	0.5709±.13	0.5470±.09	0.8111±.03	0.4722±.08	0.2245±.02	0.5092±.02	0.1635±.03	0.2070±.01	0.5027±.00	0.1551±.04
ır	GCL+FAGCN	0.6547±.04	$0.8624 \scriptstyle{\pm .01}$	$0.5667 \scriptstyle{\pm .04}$	0.7242±.03	0.6668±.00	$0.6434 {\scriptstyle \pm .07}$	0.5881±.06	$0.8756 \scriptstyle \pm .01$	$0.6183 \scriptstyle{\pm .06}$	0.2590±.02	$0.5439 \scriptstyle \pm .01$	$0.2180 \scriptstyle{\pm .01}$	0.2039±.01	$0.5077 \scriptstyle \pm .00$	$0.1558 \scriptstyle{\pm .04}$
+	Sim+GCN	0.5311±.08	$0.8151 \scriptstyle{\pm .04}$	0.4518±.09	0.6797±.05	$0.6773 \scriptstyle \pm .03$	$0.4847 {\scriptstyle \pm .06}$	0.4848±.09	$0.8138 \scriptstyle{\pm .06}$	$0.4507 \scriptstyle \pm .05$	0.2252±.02	$0.5140{\scriptstyle \pm .01}$	$0.1871 \scriptstyle{\pm .02}$	0.2062±.01	$0.5091 \scriptstyle{\pm .00}$	$0.1553 \scriptstyle{\pm .04}$
finetuning	Sim+FAGCN	0.6349±.01	$0.8876 \scriptstyle{\pm .00}$	$0.5512 \scriptstyle{\pm .01}$	0.7464±.01	$0.6750 \scriptstyle{\pm .00}$	$0.6949 \scriptstyle \pm .01$	0.5709±.09	$0.8829 \scriptstyle \pm .01$	$0.5953 \scriptstyle{\pm .07}$	0.2376±.02	$0.5251 \scriptstyle{\pm .02}$	$0.1921 \scriptstyle{\pm .02}$	0.2027±.00	$0.5109 \scriptstyle{\pm .01}$	$0.1587 \scriptstyle \pm .05$
GCOPE	GCL+GCN	0.5943±.05	0.8351±.03	0.4876±.06	0.7490±.05	0.7029±.02	0.5909±.11	0.5351±.05	0.8307±.04	0.4823±.07	0.2276±.01	0.5354±.01	0.1573±.02	0.2110±.00	0.5189±.01	0.1653±.02
GCOPE	GCL+FAGCN	0.6481±.03	$0.8545 \scriptstyle{\pm .00}$	$0.5634 \scriptstyle{\pm .02}$	0.7033±.03	$0.6554 \scriptstyle{\pm .01}$	$0.5997 \pm .04$	0.5669±.04	0.8566±.01	$0.6024 \scriptstyle{\pm .03}$	0.2442±.01	$0.5454 \scriptstyle{\pm .01}$	$0.2105 \scriptstyle{\pm .00}$	0.1985±.00	$0.5039 \scriptstyle{\pm .00}$	0.1456±.03
+	Sim+GCN	0.5726±.07	$0.8299_{\pm .05}$	$0.4283 {\scriptstyle \pm .17}$	0.7882±.04	$0.7060 \scriptstyle{\pm .01}$	0.6635±.06	0.6159±.04	0.8656±.02	$0.5810 \scriptstyle \pm .04$	0.2084±.01	$0.5039 \scriptstyle{\pm .01}$	$0.1660 {\scriptstyle \pm .03}$	0.2159±.01	$0.5135 \scriptstyle{\pm .00}$	$0.1746 \scriptstyle{\pm .02}$
finetuning	Sim+FAGCN	0.7575±.01	$0.9279 \scriptstyle \pm .00$	$0.6998 \scriptstyle{\pm .01}$	0.8105±.01	$0.7140{\scriptstyle \pm .01}$	$0.7604 \scriptstyle{\pm .01}$	0.7868±.02	$0.9237 \scriptstyle \pm .00$	$0.7490 \scriptstyle{\pm .03}$	0.2362±.02	$0.5345{\scriptstyle \pm .01}$	$0.2052 \scriptstyle{\pm .01}$	0.2037±.00	$0.5076 \scriptstyle{\pm .00}$	$0.1507 \scriptstyle{\pm .04}$
IN	ΛP(%)	4.06%	3.02%	5.34%	9.66%	4.32%	14.28%	16.76%	4.87%	15.85%	-3.60%	0.68%	-0.22%	0.38%	0.35%	-2.68%

Table A3: Cross-domain transfer learning performance (mean±std Acc/AUC/F1) on homophilic datasets (C-way-5-shot). IMP (%): the average improvement of GCOPE over the rest. GCL and Sim respectively represent GraphCL and SimGRACE.

Training	Methods		Cora			Citeseer			Pubmed			Computers			Photos	
schemes		Acc	AUC	F1	Acc	AUC	F1	Acc	AUC	F1	Acc	AUC	F1	Acc	AUC	F1
	GCN	0.6105±.03	0.8800±.03	$0.6078 \scriptstyle{\pm .04}$	0.4554±.04	$0.7478 \scriptstyle \pm .04$	$0.4361 \scriptstyle{\pm .02}$	0.6135±.02	0.7644±.03	0.5786±.05	0.4274±.05	0.8126±.03	$0.4313 \scriptstyle{\pm .03}$	0.6041±.04	0.8931±.00	$0.5817 \scriptstyle \pm .03$
supervised	GAT	0.5979±.03	$0.8652 \scriptstyle \pm .02$	$0.5727 \scriptstyle{\pm .05}$	0.5048±.02	$0.7927 \scriptstyle \pm .01$	$0.4837 \scriptstyle \pm .03$	0.6165±.01	$0.7537 \scriptstyle \pm .02$	$0.5772 \scriptstyle \pm .03$	0.5108±.04	$0.8423 \scriptstyle \pm .01$	$0.4666 {\scriptstyle \pm .04}$	0.6257±.02	0.9022±.00	$0.5936 \scriptstyle{\pm .02}$
superviseu	BWGNN	0.6502±.03	$0.8869 \scriptstyle \pm .01$	$0.6378 \scriptstyle{\pm .02}$	0.5228±.03	$0.8096 \pm .02$	$0.4886 \scriptstyle{\pm .04}$	0.5839±.02	$0.7274 \scriptstyle \pm .04$	$0.5284 {\scriptstyle \pm .05}$	0.5390±.03	$0.8483 \scriptstyle{\pm .02}$	$0.4919 \scriptstyle{\pm .04}$	0.6157±.03	0.8891±.00	$0.5839 \scriptstyle \pm .03$
	FAGCN	0.7183±.01	$0.9139 \scriptstyle \pm .01$	$0.7144{\scriptstyle \pm .01}$	0.6721±.00	0.8597±.00	$0.6390 \pm .00$	0.5965±.01	$0.7445 \scriptstyle \pm .03$	$0.5719 \scriptstyle \pm .03$	0.6054±.01	$0.8886 \scriptstyle{\pm .01}$	$0.5851 \scriptstyle{\pm .02}$	0.6655±.02	$0.9107 \scriptstyle{\pm .00}$	$0.6435 \scriptstyle \pm .01$
IΡ	GCL+GCN	0.6351±.01	0.8807±.00	0.6159±.01	0.5347±.03	0.8068±.01	0.5203±.03	0.5719±.03	0.6934±.04	0.5382±.03	0.4849±.07	0.8576±.01	0.4760±.07	0.6183±.02	0.8993±.00	0.6039±.00
ır	GCL+FAGCN	0.6948±.02	$0.9059 \scriptstyle{\pm .01}$	$0.6893 \scriptstyle{\pm .03}$	0.6768±.01	$0.8690 \pm .00$	$0.6530 \scriptstyle \pm .01$	0.6024±.01	$0.7596 \scriptstyle{\pm .02}$	$0.5876 \scriptstyle \pm .01$	0.6217±.01	$0.8806 \scriptstyle{\pm .00}$	$0.5868 \scriptstyle{\pm .00}$	0.6991±.01	$0.9083 \pm .00$	$0.6509 \scriptstyle{\pm .00}$
F	Sim+GCN	0.5596±.04	$0.8520 \scriptstyle \pm .01$	$0.5441 \scriptstyle \pm .03$	0.5180±.02	$0.7962 \pm .00$	$0.4905 \scriptstyle{\pm .03}$	0.5064±.02	$0.6503 \scriptstyle{\pm .03}$	$0.4582 {\scriptstyle \pm .06}$	0.4817±.02	$0.8464 {\scriptstyle \pm .01}$	$0.4525 \scriptstyle{\pm .02}$	0.6183±.03	0.9102±.00	$0.5964 \pm .03$
finetuning	Sim+FAGCN	0.7247±.01	$0.9183 \scriptstyle{\pm .00}$	$0.7179 \scriptstyle \pm .02$	0.6584±.01	0.8693±.00	$0.6384 \scriptstyle{\pm .01}$	0.6038±.01	$0.7467 \scriptstyle \pm .04$	0.5690±.04	0.5888±.01	$0.8749 \scriptstyle \pm .02$	$0.5505 \scriptstyle{\pm .02}$	0.6845±.02	$0.9109 \scriptstyle{\pm .00}$	$0.6380 \scriptstyle{\pm .01}$
GCOPE	GCL+GCN	0.6079±.02	0.8705±.02	0.5971±.03	0.5745±.06	0.8354±.02	0.5500±.06	0.5883±.03	0.7352±.03	0.5317±.05	0.5552±.03	0.8621±.01	0.4795±.06	0.6494±.01	0.9120±.00	0.6153±.03
GCOPE	GCL+FAGCN	0.7334±.01	$0.9247 \scriptstyle \pm .00$	$0.7238 \scriptstyle{\pm .01}$	0.6863±.02	0.8778±.00	$0.6539 {\scriptstyle \pm .02}$	0.6110±.00	$0.7552 \scriptstyle{\pm .02}$	0.5806±.01	0.6172±.01	$0.8950 \scriptstyle{\pm .00}$	$0.5969 \scriptstyle{\pm .01}$	0.6868±.00	0.9206±.00	$0.6591 \scriptstyle{\pm .00}$
+	Sim+GCN	0.5501±.02	$0.8522 \scriptstyle{\pm .01}$	$0.5298 \scriptstyle{\pm .02}$	$0.4869 \scriptstyle{\pm .01}$	$0.7884 \scriptstyle{\pm .01}$	$0.4731 \scriptstyle{\pm .02}$	0.6135±.04	$0.7684 \scriptstyle{\pm .04}$	0.5685±.06	0.5264±.00	$0.8588 \scriptstyle{\pm .01}$	$0.4928 \scriptstyle{\pm .03}$	0.6237±.03	$0.9105 \scriptstyle{\pm .00}$	$0.5759 \scriptstyle{\pm .04}$
finetuning	Sim+FAGCN	0.7313±.01	$0.9100 \scriptstyle{\pm .02}$	$0.7189 \scriptstyle \pm .01$	0.6931±.01	$0.8829 \scriptstyle \pm .00$	$0.6631 \scriptstyle{\pm .01}$	0.5754±.03	$0.7483{\scriptstyle \pm .03}$	$0.5541 \scriptstyle \pm .03$	0.6212±.02	$0.8873 \scriptstyle \pm .01$	$0.5710{\scriptstyle \pm .02}$	0.6995±.02	$0.9190 \scriptstyle{\pm .00}$	0.6544±.01
IN	IP (%)	1.05%	0.17%	0.77%	7.45%	3.33%	7.60%	1.74%	2.98%	1.38%	8.93%	2.26%	5.93%	3.66%	1.39%	2.40%

A.5 Dynamical Study of inter-coordinator edges

We additionally study the impact of dynamical inter-coordinator edges on the performance of GCOPE, and report the transfer learning results in Table A7. According to the experimental results, we observe that GCOPE/d outperforms GCOPE/f on the Wisconsin and

Texas, performs better than the supervised method on the Cora but is inferior to GCOPE/f, and exhibits negative transfer on Citeseer. In comparison, GCOPE/f demonstrates positive transfer across all datasets.

Table A4: Cross-domain transfer learning performance (mean±std Acc/AUC/F1) on heterophilic datasets (C-way-5-shot). IMP (%): the average improvement of GCOPE over the rest. GCL and Sim respectively represent GraphCL and SimGRACE.

Training	Methods		Wisconsin			Texas			Cornell			Chameleon	Į.		Squirrel	
schemes	Wellous	Acc	AUC	F1	Acc	AUC	F1	Acc	AUC	F1	Acc	AUC	F1	Acc	AUC	F1
	GCN	0.6374±.08	$0.8774_{\pm .02}$	$0.6540{\scriptstyle \pm .06}$	0.7117±.04	0.6994±.01	0.6534±.04	0.6239±.09	0.8606±.05	0.5903±.07	0.2577±.01	$0.5484 \scriptstyle{\pm .01}$	$0.2249 \scriptstyle{\pm .01}$	0.2209±.00	0.5228±.00	$0.1820 \scriptstyle{\pm .02}$
supervised	GAT	0.6128±.02	$0.8788 \scriptstyle{\pm .00}$	$0.5704 \scriptstyle{\pm .05}$	0.7517±.01	$0.6977 \scriptstyle \pm .00$	$0.6290 \scriptstyle \pm .06$	0.5549±.02	$0.8655 \scriptstyle{\pm .01}$	$0.5745 \scriptstyle \pm .05$	0.2147±.01	$0.5206 \scriptstyle{\pm .01}$	$0.2127 \scriptstyle \pm .01$	0.2083±.00	$0.5112 \scriptstyle{\pm .00}$	$0.1596 \scriptstyle{\pm .03}$
superviseu	BWGNN	0.5951±.00	$0.8745 \scriptstyle \pm .01$	$0.5902 \pm .03$	0.7628±.04	$0.7236 \scriptstyle \pm .01$	$0.6395 \scriptstyle{\pm .11}$	0.6901±.07	$0.8963 \scriptstyle{\pm .02}$	$0.6151 {\scriptstyle \pm .04}$	0.2338±.01	$0.5386 \scriptstyle{\pm .00}$	$0.1881 \scriptstyle{\pm .03}$	0.2210±.01	$0.5319 \scriptstyle \pm .01$	$0.1779 \scriptstyle \pm .03$
	FAGCN	0.5261±.03	$0.8678 \scriptstyle{\pm .02}$	$0.5074 \scriptstyle{\pm .03}$	0.7269±.02	$0.6945 \scriptstyle{\pm .01}$	$0.6734 \scriptstyle{\pm .02}$	0.5183±.02	$0.8841 \scriptstyle \pm .01$	$0.5628 \scriptstyle{\pm .03}$	0.2319±.00	$0.5212 {\scriptstyle \pm .00}$	$0.2137 \scriptstyle \pm .00$	0.2131±.00	$0.5162 \scriptstyle{\pm .01}$	$0.1863 \scriptstyle{\pm .01}$
IP	GCL+GCN	0.5941±.13	0.9031±.01	0.5893±.14	0.6331±.14	0.6858±.03	0.4816±.14	0.6141±.09	0.8478±.04	0.5050±.05	0.2500±.01	0.5253±.01	0.1685±.01	0.2144±.00	0.5181±.00	0.1821±.02
_	GCL+FAGCN	0.6039±.05	$0.9077 \scriptstyle \pm .01$	$0.5963 \scriptstyle{\pm .05}$	0.7338±.00	$0.7182 \scriptstyle \pm .01$	$0.6045 \scriptstyle{\pm .07}$	0.6930±.03	$0.9253 \scriptstyle \pm .00$	$0.6839 \scriptstyle \pm .04$	0.2319±.00	$0.5327 \scriptstyle \pm .00$	$0.2196 \scriptstyle{\pm .01}$	0.2127±.00	$0.5172 \scriptstyle \pm .00$	$0.1931 \scriptstyle{\pm .01}$
+	Sim+GCN	0.5655±.05	$0.8860 \scriptstyle{\pm .02}$	$0.5922 \pm .05$	0.7545±.01	$0.7312 \scriptstyle \pm .01$	$0.6268 \scriptstyle{\pm .05}$	0.6732±.04	$0.8717 \scriptstyle \pm .03$	$0.5895 \scriptstyle{\pm .07}$	0.2419±.01	$0.5354 \scriptstyle{\pm .00}$	$0.1832 \scriptstyle{\pm .03}$	0.2240±.00	$0.5321 \scriptstyle{\pm .01}$	$0.1890 \scriptstyle{\pm .01}$
finetuning	Sim+FAGCN	0.6739±.02	$0.9166 \scriptstyle{\pm .00}$	$0.6258 \scriptstyle{\pm .04}$	0.7352±.01	$0.7162 \scriptstyle{\pm .00}$	$0.6624 {\scriptstyle \pm .06}$	0.7634±.02	$0.9572 \scriptstyle \pm .00$	$0.7583 \scriptstyle{\pm .02}$	0.2493±.01	$0.5400 \scriptstyle{\pm .00}$	$0.2261 \scriptstyle{\pm .00}$	0.2131±.00	$0.5135{\scriptstyle \pm .00}$	$0.1764 \scriptstyle{\pm .01}$
GCOPE	GCL+GCN	0.5793±.08	0.8864±.02	0.5681±.11	0.7531±.04	0.7315±.00	0.6480±.08	0.6859±.15	0.9129±.03	0.6058±.13	0.2304±.01	0.5264±.00	0.2126±.01	0.2228±.01	0.5319±.00	0.1705±.04
GCOPE	GCL+FAGCN	0.6079±.04	$0.8971 \scriptstyle \pm .00$	$0.5870 \scriptstyle \pm .04$	0.7393±.01	$0.6989 \scriptstyle \pm .01$	$0.6736 \scriptstyle{\pm .02}$	0.6352±.03	$0.9161 \scriptstyle{\pm .00}$	$0.6302 \scriptstyle{\pm .03}$	0.2350±.00	$0.5337 \scriptstyle \pm .00$	$0.2102 \scriptstyle{\pm .01}$	0.2134±.00	$0.5220 \scriptstyle{\pm .00}$	$0.1943 \scriptstyle{\pm .00}$
+ Cti	Sim+GCN	0.6099±.06	$0.8923 \pm .01$	$0.5884 \scriptstyle{\pm .09}$	0.7407±.04	$0.7226 \scriptstyle{\pm .01}$	0.6326±.13	0.5563±.05	$0.8352 \scriptstyle \pm .05$	0.5248±.07	0.2486±.01	$0.5458 \scriptstyle{\pm .01}$	$0.1860 \scriptstyle{\pm .03}$	0.2208±.00	$0.5310 \scriptstyle{\pm .00}$	$0.1847 \scriptstyle \pm .02$
finetuning	Sim+FAGCN	0.7507±.01	$0.9478 \scriptstyle{\pm .00}$	$0.7393{\scriptstyle \pm .03}$	0.8497±.00	$0.7501 \scriptstyle{\pm .00}$	$0.8012 \scriptstyle \pm .01$	0.8437±.02	$0.9742 \scriptstyle \pm .00$	$0.8163 \scriptstyle{\pm .02}$	0.2494±.02	$0.5378 \scriptstyle{\pm .00}$	$0.2201 \scriptstyle{\pm .00}$	0.2163±.00	$0.5183 \scriptstyle{\pm .00}$	$0.1948 \scriptstyle{\pm .00}$
IN	ΛP(%)	5.96%	1.90%	5.08%	6.13%	2.46%	10.87%	6.07%	2.37%	5.63%	0.82%	0.59%	1.28%	-1.21%	1.04%	2.92%

Table A5: Cross-domain transfer learning performance (mean±std Acc/AUC/F1) on homophilic datasets (C-way-1-shot) of GCOPE with different number of graph coordinators. '-1', '-3', and '-5' represent that we assign one, three, or five graph coordinators for each dataset in GCOPE.

Methods		Cora			Citeseer			Pubmed			Computers			Photo	
Methods	Acc	AUC	F1	Acc	AUC	F1	Acc	AUC	F1	Acc	AUC	F1	Acc	AUC	F1
Supervised	0.3819±.03	0.6818±.04	0.3009±.09	0.5219±.08	0.8042±.03	$0.4667 \scriptstyle{\pm .08}$	0.4522±.02	0.5622±.04	0.4275±.07	0.4651±.04	0.7762±.02	0.3009±.07	0.5937±.05	0.8847±.00	0.5346±.03
IP	0.3892±.05	0.7228±.03	0.3619±.05	0.4461±.02	0.7781±.01	0.4126±.02	0.4532±.02	0.5708±.03	0.4168±.04	0.4371±.06	0.7616±.01	0.3450±.02	0.6273±.01	0.8710±.01	0.5406±.03
GCOPE-1	0.4618±.03	0.7597±.05	0.4388±.05	0.5631±.03	0.8258±.02	0.4953±.04	0.4591±.01	0.5512±.01	0.4203±.03	0.4465±.01	0.7747±.00	0.3432±.03	0.6329±.02	0.8850±.00	0.5935±.03
GCOPE-3	0.4272±.05	$0.7509 \scriptstyle{\pm .01}$	$0.4176 \scriptstyle{\pm .03}$	0.5518±.01	$0.8438 \scriptstyle{\pm .00}$	$0.5074 \scriptstyle{\pm .02}$	0.4777±.02	$0.5689 \scriptstyle{\pm .04}$	$0.3794 \pm .04$	0.4314±.02	$0.7335 \scriptstyle{\pm .01}$	$0.3546 \scriptstyle{\pm .00}$	0.6491±.01	$0.8934 \pm .00$	$0.6109 \scriptstyle{\pm .01}$
GCOPE-5	0.4499±.05	$0.7673 \scriptstyle{\pm .03}$	$0.4414 \scriptstyle{\pm .04}$	0.5280±.04	$0.8183 \scriptstyle{\pm .03}$	$0.4658 \scriptstyle{\pm .04}$	0.4686±.04	$0.5737 \scriptstyle{\pm .08}$	0.3663±.08	0.4650±.00	$0.7656 \scriptstyle{\pm .01}$	$0.3767 \scriptstyle{\pm .01}$	0.5538±.05	0.8760±.01	0.5621±.04

Table A6: Cross-domain transfer learning performance (mean±std Acc/AUC/F1) on heterophilic datasets (C-way-1-shot) of GCOPE with different numbers of graph coordinators. '-1', '-3', and '-5' represents the we assign one, three, or five graph coordinators for each dataset in GCOPE.

Methods	Wisconsin			Texas			Cornell			Chameleon			Squirrel		
	Acc	AUC	F1												
Supervised	0.5222±.05	0.7905±.03	0.4725±.06	0.6900±.06	0.7185±.01	0.5334±.12	0.2938±.06	0.6573±.04	0.2872±.05	0.2575±.02	0.5515±.02	0.1941±.01	0.2181±.00	0.5202±.00	0.1875±.02
IP	0.6063±.04	0.8356±.01	0.5555±.07	0.7425±.03	0.7034±.03	0.6141±.09	0.2588±.04	0.6262±.04	0.2442±.04	0.2443±.00	0.5530±.01	0.1875±.01	0.2223±.00	0.5307±.00	0.1740±.02
GCOPE-1	0.6579±.03	0.8531±.01	0.5649±.00	0.7125±.02	0.6693±.02	0.6300±.03	0.4013±.05	0.6897±.01	$0.3160 \scriptstyle{\pm .02}$	0.2886±.00	0.5898±.00	$0.2320{\scriptstyle \pm .00}$	0.2257±.00	0.5257±.00	0.1885±.01
GCOPE-3	0.6217±.00	$0.8267 \scriptstyle{\pm .00}$	$0.5397 \scriptstyle \pm .01$	0.7675±.04	$0.7005 \scriptstyle{\pm .03}$	$0.5834 \scriptstyle{\pm .05}$	0.5675±.03	$0.7334 \scriptstyle{\pm .01}$	$0.4506 \scriptstyle{\pm .02}$	0.2895±.00	$0.5785 \scriptstyle{\pm .00}$	$0.2205 \scriptstyle{\pm .00}$	0.2199±.01	$0.5274 \scriptstyle \pm .01$	$0.1815 \scriptstyle{\pm .02}$
GCOPE-5	0.6353±.06	$0.8327 \scriptstyle \pm .03$	$0.5692 \scriptstyle{\pm .05}$	0.7262±.04	$0.6913 \scriptstyle{\pm .02}$	$0.5468 \scriptstyle{\pm .04}$	0.6550±.02	$0.8350{\scriptstyle \pm .00}$	$0.5047 \scriptstyle \pm .02$	0.2810±.00	$0.5654 \scriptstyle{\pm .00}$	$0.2113 \scriptstyle{\pm .00}$	0.2129±.00	$0.5183 \scriptstyle{\pm .00}$	0.2029±.00

Table A7: Cross-domain transfer learning performance (mean±std Acc/AUC/F1) on two homophilic and two heterophilic datasets (C-way-1-shot) of GCOPE with full or dynamical inter-coordinator edges. '/f' means that the inter-coordinator edges in GCOPE are fully connected to each other. '/d' represents that inter-dataset edges in GCOPE are dynamically connected by computing the similarity between them.

Methods		Cora		Citeseer				Wisconsin		Texas		
	Acc	AUC	F1	Acc	AUC	F1	Acc	AUC	F1	Acc	AUC	F1
Supervised	0.3819±.03	0.6818±.04	0.3009±.09	0.5219±.08	0.8042±.03	0.4667±.08	0.5222±.05	0.7905±.03	0.4725±.06	0.6900±.06	0.7185±.01	0.5334±.12
GCOPE/f	0.4618±.03	0.7597±.05	0.4388±.05	0.5631±.03	0.8258±.02	0.4953±.04	0.6579±.03	0.8531±.01	$0.5649 \scriptstyle{\pm .00}$	0.7125±.02	0.6693±.02	0.6300±.03
GCOPE/d	0.4027±.00	0.7228±.01	0.4206±.00	0.4874±.04	0.7764±.03	0.4342±.04	0.6588±.01	0.8545±.00	0.6046±.02	0.7400±.03	0.6851±.02	0.5813±.05